

2014

THE NO_3^-/O_2 RESPIRATION RATIO OF THE DEEP SEDIMENTARY BIOSPHERE IN THE PACIFIC GYRES

Yiya Huang
University of Rhode Island, yiyahuang@my.uri.edu

Follow this and additional works at: <https://digitalcommons.uri.edu/theses>

Terms of Use

All rights reserved under copyright.

Recommended Citation

Huang, Yiya, "THE NO_3^-/O_2 RESPIRATION RATIO OF THE DEEP SEDIMENTARY BIOSPHERE IN THE PACIFIC GYRES" (2014). *Open Access Master's Theses*. Paper 288.
<https://digitalcommons.uri.edu/theses/288>

This Thesis is brought to you by the University of Rhode Island. It has been accepted for inclusion in Open Access Master's Theses by an authorized administrator of DigitalCommons@URI. For more information, please contact digitalcommons-group@uri.edu. For permission to reuse copyrighted content, contact the author directly.

**THE NO₃⁻/O₂ RESPIRATION RATIO OF THE DEEP SEDIMENTARY
BIOSPHERE IN THE PACIFIC GYRES**

**BY
YIYA HUANG**

**A THESIS SUBMITTED IN PARTIAL FULFILLMENT OF THE
REQUIREMENTS FOR THE DEGREE OF
MASTER OF SCIENCE
IN
OCEANOGRAPHY**

UNIVERSITY OF RHODE ISLAND

2014

MASTER OF SCIENCE THESIS

OF

YIYA HUANG

APPROVED:

Thesis Committee:

Major Professor Arthur Spivack

Steven D'Hondt

David Fastovsky

Nasser H. Zawia

DEAN OF THE GRADUATE SCHOOL

UNIVERSITY OF RHODE ISLAND

2014

ABSTRACT

Organic matter produced in the ocean has an average C/N ratio of 106:16 (the Redfield ratio). However, during transport to the seafloor, N is preferentially respired. This results in depletion of the N relative to C in the organic matter that fuels subseafloor microbial communities. It has also been argued that preferential depletion of organic N occurs in sediment. This depletion may force sedimentary microorganisms to reduce nitrate or fix dinitrogen, which requires the expenditure of a significant amount of additional energy in oxic sediment. Thus the availability of organic nitrogen may place a fundamental control on energy budget and ecosystem of the sedimentary microbial life.

We test this possibility by determining the NO_3^-/O_2 respiration ratio at three sites in the Pacific gyres. We created a diffusion-reaction model and used existing dissolved oxygen and nitrate profiles from interstitial water to determine the best-fit NO_3^-/O_2 respiration ratio. This model has an advantage over linear correlation analysis, because it explicitly considers respiration as a function of depth, and uses the curvature of the concentration profiles to determine the microbial reactions.

The down-core profiles of dissolved oxygen and nitrate reflect the net production of nitrate and consumption of oxygen due to microbial aerobic respiration. The curvature in the profiles reveals that organic nitrogen is not depleted in sedimentary organic matter respired. Dissolved nitrate and oxygen concentrations from all sites are linearly correlated with a NO_3^-/O_2 ratio of -0.098 ± 0.005 . The best-fit NO_3^-/O_2 respiration ratios calculated by the one-zone model, assuming a constant respiration ratio in the entire sediment column at each site, are between 0.089 to 0.100.

These ratios are indistinguishable from the Redfield NO_3^-/O_2 ratio of 0.094 determined in the ocean. We also consider a model to determine whether the respiration ratio varies with depth. There is no clear indication that the respiration ratio varies with sediment depth. This indicates that sedimentary microbes utilize organic carbon and nitrogen with a C/N ratio that is indistinguishable from the Redfield ratio, even though the C/N ratio of the bulk organic matter might be different due to the preferential degradation. This might be controlled by the nutrient requirements of microbial communities.

ACKNOWLEDGMENTS

I would like to express my deepest appreciation to my major advisor, Art Spivack, for his continual guidance and support during the accomplishment of this Master's thesis. His encouragement and faith in me was extremely helpful during the last two and a half years. I will always remember his patience in helping me develop the model, explaining new knowledge, and correcting my English grammatical errors.

I would like to thank Steven D'Hondt, whose C-DEBI grant (NSF-OCE 0939564) funded part of my thesis and who gave me constructive suggestions and wise insights in my research. His support motivated me to make more progress. I am very grateful to my committee member David Fastovsky for his enthusiasm and support in my Master's thesis.

I greatly thank the scientific parties of IODP Expedition 329 and Knorr 195(III), who measured all the oxygen and nitrate data. Without their data, I would not be able to work on this project. I also thank NSF and C-DEBI for funding for this project.

Many thanks to the professors in GSO: Michael Pilson, Susanne Menden-Deuer, David Smith, Rob Pockalny, and many not listed, for their assistance when I encountered problems in this project.

Great thanks to all my lab mates in Spivack and D'Hondt's lab, John, Cathleen, Emily, Justine and Mary, my officemate Kari, and all my friends at GSO for their kind help, support, and company in both my research and life.

I am especially thankful to my parents and my brother who are always supportive of my decisions. They give me the best love in the world.

PREFACE

This master's thesis is written in manuscript format as I intend to submit this work to the journal of *Limnology and Oceanography*. Following authors are involved in the publication of the manuscript:

Yiya Huang^a, Arthur J. Spivack^a, and Steven D'Hondt^a.

^a Graduate School of Oceanography, University of Rhode Island, Narragansett, RI 02882, USA.

The manuscript is currently being reviewed by co-authors involved in the project. Submission of the manuscript is estimated by summer 2014.

An appendix of the partial MATLAB code follows the manuscript to provide the reader with the information required to get a thorough understanding of the numerical model analysis in this study. I plan to make the integrated and detailed MATLAB code accessible online in form of an electronic annex upon acceptance of the manuscript. The dissolved oxygen and nitrate concentration data for Site 10 and Site 11 are also attached in the appendix. Measured data for IODP Site U1370 is available on the website of IODP Expedition 329 (<http://publications.iodp.org/proceedings/329/329toc.htm>).

TABLE OF CONTENTS

ABSTRACT	ii
ACKNOWLEDGMENTS	iv
TABLE OF CONTENTS	vi
LIST OF FIGURES	viii
LIST OF TABLES	x
INTRODUCTION	2
METHODS	5
Site locations & description	5
Dissolved oxygen and nitrate measurement	6
Dissolved O₂ and NO₃⁻ Profiles Description	7
Sediment core selection	7
Profile curvature evaluation	8
Diffusion-Reaction model analysis	10
<i>Overview of the method</i>	10
<i>Removal of outliers</i>	10
<i>Numerical model</i>	11
<i>Consideration of model settings</i>	12
<i>Consideration of boundary condition</i>	13

<i>Determination of uncertainty</i>	15
RESULTS	17
Dissolved NO₃⁻ vs. O₂	17
Evaluation of profile curvature	17
Diffusion-reaction model results	18
<i>The one-zone model</i>	18
<i>The two-zone model</i>	20
DISCUSSION	24
Profile curvatures and microbial bioenergetics	24
Dissolved nitrate vs. dissolved oxygen	27
Diffusion-Reaction model analysis	29
<i>The one-zone model</i>	29
<i>The two-zone model</i>	29
SUMMARY	32
LIST OF REFERENCES	33
FIGURES	37
TABLES	57
APPENDIX	60

LIST OF FIGURES

FIGURE	PAGE
Figure 1 Location of Knorr Site 10 and Site 11 in the North Pacific Gyre and IODP Site U1370 in the South Pacific Gyre.	37
Figure 2.1 Dissolved oxygen and nitrate profiles in the interstitial water collected from multiple sediment cores at Site 10	38
Figure 2.2 Dissolved oxygen and nitrate profiles in the interstitial water collected from multiple sediment cores at Site 11.	39
Figure 2.3 Dissolved oxygen and nitrate profiles in the interstitial water collected from multiple sediment holes at Site U1370	40
Figure 3.1 Dissolved oxygen and nitrate profiles of selected sediment cores at Site 10 used in model analysis	41
Figure 3.2 Dissolved oxygen and nitrate profiles of selected sediment cores at Site 11 used in model analysis	42
Figure 3.3 Dissolved oxygen and nitrate profiles of selected sediment cores at Site U1370 used in model analysis	43
Figure 4 The diagram of the two cases of the boundary conditions in the two-zone model.....	44
Figure 5 The dissolved nitrate versus dissolved oxygen in interstitial water from all sites.....	45
Figure 6.1 The best-fit curves (red line) for oxygen and nitrate profiles at Site 10 (A) and Site 11 (B) in the one-zone model (Conc. BC)	46

Figure 6.2 The best-fit curves (red line) for oxygen and nitrate profiles at Site U1370 in the one-zone model (Conc. BC).....	47
Figure 7.1 The best-fit curves (red line) for oxygen and nitrate profiles at Site 10 (A) and Site 11 (B) in the one-zone model (Flux BC)	48
Figure 7.2 The best-fit curves (red line) for oxygen and nitrate profiles at Site U1370 in the one-zone model (Flux BC).....	49
Figure 8 The best-fit NO_3^-/O_2 respiration ratios determined by the one-zone model analysis at each site (Conc. BC & Flux BC).....	50
Figure 9.1 The best-fit oxygen and nitrate profiles at Site 10 in the two-zone model (Conc. BC for the deeper zone)	51
Figure 9.2 The best-fit oxygen and nitrate profiles at Site 11 in the two-zone model (Conc. BC for the deeper zone).	52
Figure 9.3 The best-fit oxygen and nitrate profiles at Site U1370 in the two-zone model (Conc. BC for the deeper zone)	53
Figure 10.1 The best-fit oxygen and nitrate profiles at Site 10 in the two-zone model (Flux BC for the deeper zone).....	54
Figure 10.2 The best-fit oxygen and nitrate profiles at Site 11 in the two-zone model (Flux BC for the deeper zone).....	55
Figure 10.3 The best-fit oxygen and nitrate profiles at Site U1370 in the two-zone model (Flux BC for the deeper zone).....	56

LIST OF TABLES

TABLE	PAGE
Table 1 The location and the water depth of the sediment sample sites	57
Table 2 The best-fit NO ₃ ⁻ /-O ₂ respiration ratio and the referred C/N ratio from the one-zone model at each site, using both Conc. BC and Flux BC. The uncertainty of NO ₃ ⁻ /-O ₂ respiration ratio is of 95% confidence level. The referred C/N is calculated based on the NO ₃ ⁻ /-O ₂ respiration ratio and the average carbon oxidation state of 0 (R.K.R, 1963), shown in italics, and -0.7 (Hedges <i>et al.</i> , 2002), shown in parenthesis. The C/N/-O ₂ ratios from pervious studies are also listed for comparison.....	58
Table 3 The best-fit NO ₃ ⁻ /-O ₂ respiration ratio from the two-zone model at each site. The boundary between the two zones is placed at the depth where the change of oxygen concentration is calculated including the bottom water value (r*) or excluding the bottom water value (r**). Only Conc. BC is used for the upper zone, and Conc. BC (A) and Flux BC (B) are considered for the deeper zone... .	59

“The NO_3^-/O_2 Respiration Ratio of The Deep Sedimentary Biosphere in The Pacific Gyres”

by

Yiya Huang^a, Arthur J. Spivack^a, Steven D’Hondt^a

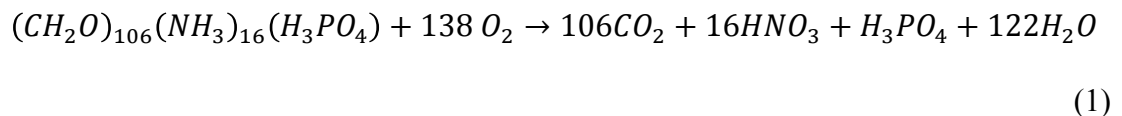
The manuscript is currently being reviewed by co-authors and is to be submitted for publication in *Limnology and Oceanography*.

^a Graduate School of Oceanography, University of Rhode Island, Narragansett, RI 02882, USA.

INTRODUCTION

Microbial life has been identified in various natural environments, including ancient deep seafloor sediments (Parkes *et al.*, 2000; D'Hondt *et al.*, 2004; Røy *et al.*, 2012). Biogenic detrital organic matter in the sediment is the primary nutrient and energy source for most deep seafloor microbial communities (D'Hondt *et al.*, 2004). In oxic sediment, microbial aerobic respiration occurs. The chemical composition of the organic matter strongly impacts microbial respiration and energy utilization, which further profoundly influence the structure of deep seafloor microbial communities. However, little is known about the impact of the sedimentary organic matter composition on microbial respiration reactions. In this study, we investigate the nitrogen content of the organic matter respired during aerobic respiration and its influence on microbial bioenergetics in deep-sea sediment.

The primary source of the organic matter in the pelagic sediment is phytoplankton debris from the upper ocean (Burdige, 2006). In 1934, Redfield found that the C/N/P ratio of planktons is 106:16:1 and is spatially constant in the ocean. This ratio is referred as the Redfield ratio. The aerobic respiration of Redfieldian organic matter can be simply expressed by the traditional Redfield-Ketchum-Richards (R.K.R) equation (Redfield *et al.*, 1963):



This equation gives the NO_3^-/O_2 respiration ratio, which is defined as the ratio of NO_3^- production to O_2 consumption. The NO_3^-/O_2 respiration ratio depends on the C/N ratio and the oxidation state of carbon of the organic matter respired.

In the 1963 formulation of Redfield *et al.*, the NO_3^-/O_2 respiration ratio for organic matter is 16/138 (0.116). However, based on the covariance of dissolved NO_3^- and O_2 throughout much of the ocean, the NO_3^-/O_2 ratio has been revised to 16/172 (0.093) (Takahashi *et al.*, 1985) and 16/170 (0.094) (Anderson and Sarmiento, 1994).

During transport to the seafloor, organic matter undergoes strong preferential degradation of N-containing compounds (Bishop *et al.*, 1977; Knauer *et al.*, 1979; Honjo, 1980). This means that proteins and nucleic acids, the primary N-containing compounds in biomolecules, are preferentially degraded relative to carbohydrates and lipids, which are major N-deficient compounds in marine organic matter. As a result, the C/N ratio of sinking organic matter increases with water depth, implying that the organic matter supplied to sediment is depleted in N relative to the Redfieldian organic matter. The C/N ratio of sedimentary organic matter in anoxic sediment has also been reported to increase with sediment depth, indicating that preferential degradation of N-rich compounds also occurs in subseafloor sediment (Arrhenius, 1953; Barreto *et al.*, 1975; Da Rocha *et al.*, 1975).

With continuous preferential degradation, as in the conventional view, organic nitrogen will be depleted faster than carbon in sedimentary organic matter. Such preferential depletion of organic nitrogen would strongly impact microbial energy budgets, as microorganisms might have to reduce inorganic N as their nitrogen source,

which is energetically costly. This may be of particular importance in deep subseafloor sediment, where energy limitation is extreme.

As in the water column, the sedimentary NO_3^-/O_2 respiration ratio reflects the C/N ratio of organic matter consumed during aerobic respiration. It can thus be used to indicate the availability of the nitrogen in sedimentary organic matter and whether microorganisms must pay a N-reduction tax.

Grundmanis and Murray (1982) analyzed dissolved nitrate and oxygen in interstitial water in shallow Equatorial Pacific sediments and found an average ratio of dissolved nitrate to dissolved oxygen of 12:130 (0.092), and C/N ratio of decomposing organic matter of 8.5 ± 1.6 , which is similar to the classic Redfield ratio of 6.6. In the northeast Pacific, Murray & Kuivila (1990) observed a NO_3^-/O_2 ratio of -0.087. The sediment cores they analyzed, however, only penetrated 50 cm below the seafloor and the respiration ratio below that depth remains unknown. The sediment beneath the Pacific gyres is oxygenated for tens of meters below the seafloor (Røy *et al.*, 2012), leaving a vast region of Earth's biosphere for which there is no information about the respiration. Analysis of the NO_3^-/O_2 respiration ratio in deeper sediment cores is therefore needed.

Here, we analyze dissolved oxygen and nitrate profiles in interstitial water of long sediment cores collected in the North and South Pacific gyres, and infer the availability of reduced nitrogen in the organic matter consumed during aerobic respiration. We use a diffusion-reaction model to calculate the best-fit NO_3^-/O_2 respiration ratio and examine its variation with sediment depth in deep subseafloor sediments.

METHODS

Site locations & description

All data are from three sites in the Pacific gyres (Table 1; Figure 1). We selected these three sites because dissolved oxygen penetrates throughout the entire recovered sediment column at all sites (Expedition 329 Scientists, 2011a; Røy *et al.*, 2012).

Site 10 (20°41'N, 143°21'W, 5410 m water depth) and Site 11 (30°21'N, 157°52'W, 5819 m water depth) were cored during R/V Knorr Expedition 195(III) in the equatorial Pacific and North Pacific Gyre (January – February 2009). The estimated basement depth is between 35 to 100 meters below the seafloor (mbsf) at Site 10 and the estimated basement age is about 68.5 Ma (Becker *et al.*, 2009). At Site 11, the estimated basement depth is 40 to 100 mbsf and its age is estimated to be about 88.7 Ma (Becker *et al.*, 2009). Site 11 is at the same location as a well-studied previously retrieved core, GPC-3. The Cretaceous/Paleogene boundary (65.5 Ma) is at 20 meters below seafloor in GPC-3, which provides an accurate and precise age estimate for Site 11 (Kyte & Wasson, 1986).

Site U1370 (40°51'S, 153°06'W, 5074 meters water depth) was cored during Integrated Ocean Drilling Program (IODP) Expedition 329 to the South Pacific Gyre (October – December 2010) (Expedition 329 Scientists, 2011a). This site is within magnetic polarity Chron 33n, giving a crustal age from 73.6 to 79.5 Ma (Gradstein *et al.*, 2004). The tectonic reconstruction of the region revealed that the crust was accreted along the Pacific-Phoenix spreading center at approximately 75 Ma (Larson

et al., 2002). The sediment column is approximately 70 meters thick (Expedition 329 Scientists, 2011a).

Dissolved oxygen and nitrate measurement

Dissolved oxygen concentrations were measured with fiber-optic oxygen microsensors, i.e. optodes, on capped and sealed 1.5 m whole-round core sections by shipboard scientists (Expedition 329 Scientists, 2011b; Røy *et al.*, 2012). Optode measurements were at 10-50 cm depth intervals for the uppermost 3 mbsf and 50 cm intervals at greater depths. The optodes were calibrated in sodium sulfite (Na_2SO_3)-saturated filtered seawater (0%) and water-saturated air (100%). The standard deviation on optode measurements was <0.3% (Expedition 329 Scientists, 2011b).

Dissolved nitrate concentration was measured using interstitial water extracted using Rhizon™ Soil Moisture Samplers (Rhizosphere Research Products, Wageningen, The Netherlands) by suction filtering through thin tubes of hydrophilic porous polymer with a mean pore diameter of 0.1 μm (Gribsholt and Kristensen, 2002, Schrum *et al.*, 2009). This method allows to effectively detecting even the lowest concentration of nitrate (<1 $\mu\text{mol L}^{-1}$) (Expedition 329 Scientists, 2011b). Nitrate concentrations were determined with a Metrohm 844 UV/VIS Compact ion chromatograph. A 50 $\mu\text{mol L}^{-1}$ sodium nitrate/nitrite standard was run after every second, third, or fourth sample depending on instrument stability. The 50 $\mu\text{mol L}^{-1}$ standard was calibrated with CRM 104–certified reference material obtained from the laboratory of Professor Andrew Dickson, Marine Physical Laboratory, Scripps Institution of Oceanography (Expedition 329 Scientists, 2011b).

Dissolved O₂ and NO₃⁻ Profiles Description

Oxygen penetrates the entire depth interval to 26.3 mbsf at Site 10, and 28.58 mbsf at Site 11 (Figure 2.1, 2.2). At Site U1370, oxygen also penetrates the whole sediment sequence to 68 mbsf (Figure 2.3; Expedition 329 Scientists, 2011a).

At all three sites, oxygen decreases with sediment depth (Figure 2.1-2.3). The decrease is very strong in the shallowest sediment and becomes more gradual with increasing sediment depth. Nitrate profiles appear to have relatively greater scatter than the oxygen profiles due to their smaller range. Although the measurement precision for oxygen and nitrate are similar, the smaller range leads to a bigger uncertainty in the change in nitrate. Despite this, nitrate profiles still show a clear and well-resolved increase with depth, indicating there is nitrate production in the sediment from microbial aerobic respiration. At Site U1370, however, nitrate decreases slightly below 50 meters (Expedition 329 Scientists, 2011a), which is probably caused by deeper consumption or diffusion into the basement.

At each site, the bottom water concentrations of oxygen and nitrate were acquired from the World Ocean Circulation Experiment (WOCE) Atlas Pacific volume 2.

Sediment core selection

Multiple types of sediment cores were collected at Site 10 and Site 11, including gravity core, multi-core and long piston core. Sediment depth adjustments were performed before numerical model analysis, if necessary, to fix the depth offsets. Oxygen and nitrate concentrations may not be measured on the same core. Taking this into account and based on the recovery depth and the quality of the measurements of

each core, gravity core GC-2 and long piston core LC-2 at Site 10 are not included in the numerical model analysis. As a result, at this site, we use gravity core GC-1, long piston core LC-1 and multicore MC in our analysis (Figure 3.1). Similarly, only gravity core GC-1, long core LC-1 and multicore MC were selected for model analysis for Site 11 (Figure 3.2).

For IODP Site U1370, only piston cores were collected, however, multiple holes were drilled (Figure 3.3; Expedition 329 Scientists, 2011a). Due to the short depth recovery, we do not use U1370 Hole F. The oxygen profile of U1370 Hole E appears to be offset about 2 meters above the profile of Hole D. The sediment core log suggests that there might be sediment missing at the top of Hole E. To account for this possibly missing sediment, we adjusted the depth of both oxygen and nitrate profiles of Hole E by adding 2 meters to the measured depths, which results in a good matching between the adjusted oxygen profile of Hole E and the oxygen profiles from other holes. However, after adjustment, the nitrate profile of Hole E was not consistent with that of Hole B between 1 mbsf to 7.5 mbsf, as shown in Figure 3.3. We use both depth scales (unadjusted depth and adjusted depth for Hole E) for Site U1370 in the model analysis.

Profile curvature evaluation

In general, the nitrate profiles looks like the mirror images of the oxygen profiles at each site: oxygen decreases with depth while nitrate increases. The changes of oxygen and nitrate concentration with depth may be the effect of only diffusion or both diffusion and microbial reactions. To determine the extent of oxygen

consumption and nitrate production in the sediment, we evaluated the curvature of each concentration profile in the following manner.

The curvature of both oxygen and nitrate profiles is maximal at shallower sediments and decreases with depth, becoming undetectable at greater depths. To quantitatively evaluate the curvature, we applied an F-test to both oxygen and nitrate profiles. From the end of the profile, we chose n data points. We used a linear regression and a quadratic regression to fit these n data points, and calculated the sum of square error (SSE) of each regression. We then determined the F value and compared it to the standard F distribution table ($\alpha=0.05$, $df = n-3$). Our null hypothesis is that a quadratic regression is not significantly better than a linear regression to fit these n data points. If the F value is smaller than the standard F value, the null hypothesis is accepted. Then we added the data point right above those n points and selected a total of $n+1$ data points. We then repeated the regressions and F-test ($\alpha=0.05$, $df = n-2$) on these $n+1$ points. We repeated this process until the calculated F value of the chosen data was bigger than the standard F value. At this endpoint, the quadratic regression fitted the data significantly better than the linear regression. Significant curvature occurs above the depth where the null hypothesis was not true. This approach limits the depth of our analysis to depths where the change in oxygen concentration is large enough to cause a measurable change in nitrate concentration that is measurable.

Diffusion-Reaction model analysis

Overview of the method

The aim of our diffusion-reaction model analysis is to find the NO_3^-/O_2 respiration ratio that best fits the measured data. Toward this end, we calculate O_2 consumption rates as a function of depth directly from the dissolved oxygen profile. We then predicted the nitrate production rates and nitrate concentrations at different depths from the O_2 consumption rates, in which the NO_3^-/O_2 respiration ratio is an adjustable parameter connecting the oxygen consumption and nitrate production during microbial aerobic respiration. We determined the best-fit NO_3^-/O_2 respiration ratio by minimizing the difference between measured and predicted nitrate values. We then applied a Monte Carlo method to estimate the uncertainty of NO_3^-/O_2 respiration ratio due to chemical analytical/sampling errors (Wang *et al.*, 2008).

Removal of outliers

In general, the dissolved oxygen and nitrate concentrations measured at all of the three sites are of high spatial resolution throughout the sediment column (Knorr 195(III) Shipboard Scientists, 2009; Expedition 329 Scientists, 2011a). To eliminate the influence of outliers, we smoothed the data using the LOWESS function (locally weighted scatter plot smoothing, 50%). We then determined the standard deviation of the absolute difference between measured data and removed the significant outliers, which are two or more standard deviations different from the smoothed profile. This approach insures that all the data points included in this study are within reliable analytical uncertainties.

Numerical model

In sedimentary interstitial water, at steady state, the mass balance of dissolved oxygen or nitrate in one dimension (depth) can be expressed mathematically as

$$-\frac{\partial}{\partial z} \left(\frac{D\phi}{\theta^2} \frac{\partial}{\partial z} C(z) \right) + R(z) = 0 \quad (2)$$

where $C(z)$ indicates either oxygen or nitrate concentration ($\mu\text{mol L}^{-1}$) as a function of sediment depth z (m, positive downward), D is the molecular diffusion coefficient ($\text{m}^2 \text{yr}^{-1}$), ϕ is the sediment porosity (unitless), θ^2 is the sediment tortuosity (unitless), and $R(z)$ represents the rate of biological reactions ($\mu\text{mol}\cdot\text{L}^{-1} \text{yr}^{-1}$). In equation (1), no advection is considered, because the advection is much smaller than diffusion at these sites.

Based on Equation (2), the mass balance equation for oxygen at steady state is as follows

$$-\frac{\partial}{\partial z} \left(\frac{D_{O_2}\phi}{\theta^2} \frac{\partial}{\partial z} [O_2] \right) + R_{O_2}(z) = 0 \quad (3)$$

Rearranging Equation (3), the oxygen consumption rate can be expressed as

$$R_{O_2}(z) = \frac{\partial}{\partial z} \left(\frac{D_{O_2}\phi}{\theta^2} \frac{\partial}{\partial z} [O_2] \right) \quad (3)$$

We interpolated measured oxygen concentrations to constant depth intervals (0.025 m).

At each even depth, we calculated oxygen consumption rate $R_{O_2}(z)$ by finite difference approximation of equation (4)

$$R_{O_2}(z) = \frac{D_{O_2}\phi}{\theta^2} \frac{([O_2]_{z+1} - 2 * [O_2]_z + [O_2]_{z-1})}{(\Delta z)^2} \quad (4)$$

assuming D , ϕ , θ^2 are constant with sediment depth. At Sites 10,11 and U1370, the temperature variation with depth is very small and D , ϕ , θ^2 are nearly constant over the depth we considered (Lado Insua, 2013). In this model analysis, we use $D_{O_2} =$

$6.0 \times 10^{-6} \text{ cm}^2 \text{ s}^{-1}$, $D_{NO_3^-} = 4.92 \times 10^{-6} \text{ cm}^2 \text{ s}^{-1}$ as the diffusion coefficient for dissolved oxygen and nitrate, respectively (Murray & Grundmanis, 1980, Schulz & Zabel, 2006).

Based on the calculated oxygen consumption rate from equation (4), the predicted nitrate production rate is

$$R_{NO_3^-}(z) = \frac{D_{NO_3^-} \theta}{\theta^2} \frac{([NO_3^-]_{z+1} - 2 * [NO_3^-]_z + [NO_3^-]_{z-1})}{(\Delta z)^2} = R_{O_2}(z) * r \quad (5)$$

where r is the NO_3^-/O_2 respiration ratio, which is an adjustable parameter for every depth. Rearranging the above equation

$$\frac{\partial^2}{\partial z^2} [NO_3^-] = \frac{([NO_3^-]_{z+1} - 2 * [NO_3^-]_z + [NO_3^-]_{z-1})}{(\Delta z)^2} = \frac{\theta^2}{D_{NO_3^-} \theta} * r * R_{O_2}(z) \quad (6)$$

We then calculated nitrate concentrations and interpolated them to depths of the nitrate measurements. We estimated the sum of square error (SSE) between $[NO_3^-]_{measured}$ and $[NO_3^-]_{calculated}$ and minimized it using a least-square method. By adjusting the NO_3^-/O_2 respiration ratio to minimize the SSE, we found the best-fit NO_3^-/O_2 respiration ratio.

At the same time, the model also predicts an oxygen profile. The predicted oxygen profile should fit with the measured profile perfectly if the model works well. This is because the predicted oxygen profile is calculated based on the oxygen consumption rate, which is the curvature of the measured oxygen profile. We used the predicted oxygen profile to test the internal consistency of the model.

Consideration of model settings

We considered two model cases to examine the variation of the NO_3^-/O_2 respiration ratio with depth. We refer to these as the one-zone model and the two-zone model. In the one-zone model, we assumed that the NO_3^-/O_2 respiration ratio is

constant with sediment depth in the entire sediment interval under consideration. If the respiration ratio varies significantly with depth, we expect a poor fit to the measured data. In the two-zone model, we separated the sediment core into two zones, each zone with a constant and independent respiration ratio. The two-zone model is aimed to evaluate the range of the variation of the NO_3^-/O_2 respiration ratio with sediment depth.

In the two-zone model, we used the depth where the oxygen concentration depletion is half of the total change as the boundary between two zones. This boundary is chosen so that each zone has approximately the same signal/noise ratio. Whether or not the bottom water concentration is included when calculating the total oxygen change can potentially create an artifact, in particular at Site U1370, due to the large concentration difference between the bottom water concentration and the shallowest sediment sample measured. This difference is most likely due to loss of sediment at the core top during the coring process or sediment recovery. To address this problem, we ran the analysis two different ways; we placed the boundary at the depth where the change of oxygen concentration is calculated including (denoted as *boundary depth I*) and excluding (denoted as *boundary depth II*) the bottom water value.

Consideration of boundary condition

In the one-zone model, we considered two cases for the boundary conditions in the numerical model analysis. In the first case, we used concentrations of oxygen and nitrate in bottom water (WOCE Atlas Volume 2: Pacific Ocean) at the sample site as the top boundary condition, and the concentrations of the deepest sample from the

LOWESS smooth curve as the bottom boundary condition. We refer to this case as concentration boundary condition (Conc. BC). In the second case, we used the same top concentration boundary condition as in the Conc. BC, but for the bottom boundary, instead of using concentration, we used the diffusive flux as boundary condition. We refer to this case as flux boundary condition (Flux BC).

The numerical model for each boundary condition case is:

Case 1: Conc. BC:

Equation (6) is formulated in matrix notation as

$$\begin{bmatrix} [NO_3^-]_{z_2} \\ [NO_3^-]_{z_3} \\ \vdots \\ [NO_3^-]_{z_{n-1}} \end{bmatrix} = \begin{bmatrix} -2 & 1 & & & & & \\ 1 & -2 & 1 & & & & \\ & & & \dots & & & \\ & & & & 1 & -2 & 1 \\ & & & & & 1 & -2 \end{bmatrix}^{-1} \begin{bmatrix} \frac{(\Delta z)^2 \theta^2}{D_{NO_3^-} - \phi} r_{z_2} * R_{O_2}(z_2) - [NO_3^-]_{z_1} \\ \frac{(\Delta z)^2 \theta^2}{D_{NO_3^-} - \phi} r_{z_3} * R_{O_2}(z_3) \\ \vdots \\ \frac{(\Delta z)^2 \theta^2}{D_{NO_3^-} - \phi} r_{z_2} * R_{O_2}(z_{n-1}) - [NO_3^-]_{z_n} \end{bmatrix} \quad (7)$$

Case 2: Flux BC:

Equation (6) is formulated in matrix notation as

$$\begin{bmatrix} [NO_3^-]_{z2} \\ [NO_3^-]_{z3} \\ \vdots \\ [NO_3^-]_{zn-1} \\ [NO_3^-]_{zn} \end{bmatrix} = \begin{bmatrix} -2 & 1 & & & & & \\ 1 & -2 & 1 & & & & \\ & & & \dots & & & \\ & & & & 1 & -2 & 1 \\ & & & & & 1 & -1 \end{bmatrix}^{-1} \begin{bmatrix} \frac{(\Delta z)^2 \theta^2}{D_{NO_3^-} \phi} r_{z2} * R_{O_2}(z_2) - [NO_3^-]_{z1} \\ \frac{(\Delta z)^2 \theta^2}{D_{NO_3^-} \phi} r_{z3} * R_{O_2}(z_3) \\ \vdots \\ \frac{(\Delta z)^2 \theta^2}{D_{NO_3^-} \phi} r_{z2} * R_{O_2}(z_{n-1}) - [NO_3^-]_{zn} \\ [O_2]_{zn} - [O_2]_{zn-1} \end{bmatrix} \quad (8)$$

In the two-zone model, we only used the Conc. BC for the upper zone but considered two boundary conditions, the Conc. BC and the Flux BC, for the deeper zone. We only used the Conc. BC for the upper zone, instead of Flux BC, because the concentration boundary condition makes the predicted profile continuous between two zones (Figure 4).

Determination of uncertainty

We separately considered (i) uncertainty due to sampling and chemical analysis (data uncertainty) and (ii) the uncertainty due to the choice of the boundary conditions of the model (BC uncertainty).

To evaluate the data uncertainty of estimated NO_3^-/O_2 respiration ratio, we applied a Monte Carlo method. We calculated a relative standard deviation based on the difference between measured concentrations and the smoothed concentration profile (see above). This relative standard deviation represents the overall method

error. The assumption is that deviations from a smooth profile allow the estimation of data uncertainty because the data should smoothly vary *in situ* due to diffusion.

To generate a representative randomized profile for the Monte Carlo analysis, we first randomly generated a group of numbers from a standard normal distribution $N(0,1)$ and then used it to generate the randomized profiles

$$C_r = C_s * (1 + \varepsilon * rn) \quad (9)$$

where ε is the relative deviation between measured data and smoothed data, rn is the random number, C_r is the randomized data and C_s are the LOWESS smoothed data.

Repeating the same procedures, each set of randomized concentration profiles is applied in the model calculation, and used to find a best-fit NO_3^-/O_2 respiration ratio. For this study, we (i) ran one hundred Monte Carlo simulations at each sample site using each boundary condition case and (ii) then estimated the standard deviation of the NO_3^-/O_2 respiration ratios from each run. We take this as the uncertainty due to the sampling/analytical error on the estimated NO_3^-/O_2 respiration ratio.

To evaluate the BC uncertainty, we compared the difference between the estimated NO_3^-/O_2 respiration ratios using different boundary conditions in the same model. In two-zone case, moreover, we also estimated the uncertainty caused by the boundary depth between two zones. We used the difference between the calculated ratios using different boundary depth for this uncertainty.

RESULTS

Dissolved NO_3^- vs. O_2

Nitrate and oxygen concentrations are generally linearly correlated for all sites. However, at low oxygen concentrations, nitrate negatively deviates from the linear trend (Figure 5). This deviation may be due to a diffusive flux into the basement or to sediment denitrification. In the linear section, the data trend are similar to the Redfield ratio derived from the water column, as given in the red line in Figure 5 (Takahashi et, 1985, Anderson and Sarmiento, 1994). Curvature in the profiles solely reflects microbial nitrate production and oxygen consumption (assuming the tortuosity and diffusion coefficient do not significantly vary with sediment depth). We use the concentration profile curvature in the intervals where there is no denitrification (based on oxygen concentrations) to identify in-situ reaction rates and the associated respiration ratio.

Evaluation of profile curvature

At Site U1370, below the depth of 50 mbsf, the oxygen concentration slightly decreases with depth to below $8 \mu\text{M}$, which is the oxygen level generally regarded below which denitrification may occur (Devol, 1978). Therefore, we only analyze the sediment above 50 mbsf at this site.

The oxygen profiles of all three sites present a negative and concave-upward curvature, which indicates consumption of oxygen. In contrast, the positive curvature of the nitrate profiles indicates production of nitrate in the sediment. Both oxygen and nitrate profiles exhibit decreasing curvature with sediment depth, indicating that the

rates of aerobic respiration and nitrate production decrease with increasing depth. We used an F-test to evaluate the curvature of the profile and limit the depth of the analysis to depths where the change in oxygen concentration is large enough to cause a change in nitrate concentration that is measurable. Detectable curvature in the oxygen profile exists to a depth of 14.2 m, 19.8 m and 39.8 m (41.8 m for adapted depth) at Site 10, Site 11 and Site U1370, respectively. At the depths where oxygen curvature is detected, there also is significant nitrate curvature. Curvature can be detected in sediment up to the following ages: 10-28 Ma for Site 10, 65 Ma for Site 11, and 42-44 Ma for Site U1370. These age estimates are based on sedimentation rate at each site, which was calculated using the age and depth of the basement for Sites 10 and U1370 (Becker *et al.*, 2009) and the age and depth of the Cretaceous/Paleogene boundary impact layer for Site 11 (Kyte & Wasson, 1986).

Diffusion-reaction model results

The one-zone model

The model-fit profiles, shown as red curves in Figure 6 (for Conc. BC) and Figure 7 (for Flux BC), are plotted with the measured values. The model-fit oxygen profiles at all sites exactly fit the measured oxygen profiles, indicating that our model is internally consistent. Additionally, the model-fit nitrate profiles are very similar to the measured profiles, demonstrating that nitrate concentrations are accurately predicted by our model and the NO_3^-/O_2 respiration ratio is correctly determined. The assumption of constant NO_3^-/O_2 respiration ratio with depth is valid.

The calculated best-fit NO_3^-/O_2 respiration ratio, for the one-zone model at each site is given in Table 2. Using the Conc. BC, the best-fit NO_3^-/O_2 respiration

ratio at Site 10, Site 11 and Site U1370 is 0.089 ± 0.004 , 0.100 ± 0.003 and 0.098 ± 0.004 , respectively, with a mean of 0.096 ± 0.003 (95% confidence level based on Monte Carlo simulations). Using the Flux BC, the best-fit NO_3^-/O_2 respiration ratio at Site 10, Site 11 and Site U1370 is 0.094 ± 0.002 , 0.092 ± 0.001 and 0.090 ± 0.002 , respectively. The mean of the NO_3^-/O_2 respiration ratio at all three sites is 0.092 ± 0.002 (95% confidence level). The calculated ratios only vary slightly between sites, no matter which boundary condition is used.

As mentioned in a previous subsection, two groups of data for Site U1370, the depth-unadjusted profiles (unadjusted profiles) and the depth-adjusted profiles (adjusted profiles) of oxygen and nitrate in Hole E, are used in the one-zone model. When using unadjusted profiles, the best-fit ratio is -0.098 using Conc. BC and -0.090 using Flux BC. When using the adjusted profiles, the best-fit ratio is -0.090 using Conc. BC and -0.087 using Flux BC (Figure 6.2 & 7.2). The difference between the NO_3^-/O_2 respiration ratios using the two different groups of data is relatively small (about 9% in the case of Conc. BC and 3% in the case of Flux BC). We therefore use the unadjusted profile of Hole E for the remaining analysis.

The average oxidation state of carbon in marine organic matter is generally thought to be either zero, as in the R.K.R equation, or between -0.3 and -0.7 (Hedges *et al.*, 2002). We used the range of 0 to -0.7 for the carbon oxidation state to infer the C/N ratio of the organic matter respired. The calculated C/N ratios at all sites are within the range of 7 to 9, which is very similar to ratios in the literature (Table 3; Grundmanis and Murray, 1982; Takahashi *et al.*, 1985; Anderson and Sarmiento, 1994).

The calculated NO_3^-/O_2 respiration ratios from our model analysis are shown in Figure 8. The error bars indicate the data uncertainty due to the chemical analysis and sampling process, which is estimated by the Monte Carlo simulations. This data uncertainty is less than 5% of the calculated NO_3^-/O_2 respiration ratio using Conc. BC, and 3% using Flux BC. These small uncertainties indicate that the errors associated with the chemical analysis and sampling methods are almost negligible.

We also estimated the uncertainty of the NO_3^-/O_2 respiration ratio due to application of different boundary conditions in the model (BC uncertainty). We base this estimate on the difference in the best-fit ratio between the two cases. The uncertainty is 5%, 8% and 9% at Site 10, Site 11 and Site U1370, respectively. The data uncertainty is almost the same magnitude as the BC uncertainty at Site 10. However, at Site 11 and Site U1370, the BC uncertainties are about two-fold larger. This indicates that the BC uncertainty has a larger effect than the data uncertainty. However, all of the uncertainties are within 10%.

Within 10%, no matter which boundary condition is used, the NO_3^-/O_2 respiration ratios at the different sites are very similar and cannot be distinguished. The modeled NO_3^-/O_2 respiration ratios are very close to the linear slope, -0.098, of the N/O_2 correlation (Figure 5).

The two-zone model

We also used the two-zone model to evaluate the range of the variation of the NO_3^-/O_2 respiration ratio at each site (Table 3; Figure 9 & 10). As previously described for the one-zone model, both Conc. BC and Flux BC are considered for the deeper zone while only the Conc. BC is used in the upper zone (Figure 4).

Site 10

The best-fit NO_3^-/O_2 respiration ratio for the upper zone is 0.0855 ± 0.0005 , where the uncertainty covers the range of the respiration ratio due to the choice of the boundary depth between the two zones (boundary depth *I* or *II*). The calculated respiration ratios for the deeper zone are 0.119 ± 0.002 using the Conc. BC, and 0.111 ± 0.003 using the Flux BC. At this site, for both zones, the calculated respiration ratios are not sensitive to the choice of boundary depth: the relative uncertainty range is less than 6 %. The choice of different boundary conditions (Conc. BC or Flux BC) in the deeper zone produces a relative uncertainty range of ~ 10 %.

The best-fit NO_3^-/O_2 respiration ratio for the one-zone model at this site, 0.089 ± 0.004 using Conc. BC and 0.094 ± 0.002 using Flux BC, is bracketed by the ratios calculated in the two-zone model, as is expected. The calculated respiration ratio in the upper zone of the two-zone model is very similar to the ratio in the one-zone model and the Redfield ratio (~ 10 % difference). However, the respiration ratio calculated in the deeper zone is ~ 30 % higher than the ratio estimated by the one-zone model.

Site 11

The best-fit respiration ratio in the upper zone is 0.148 ± 0.003 , which is almost 50% higher than the ratio calculated in the one-zone model. The reason for such a large difference is the limited spatial resolution of the data. As shown in Figure 9.2 & 10.2, there are two data gaps in the upper zone of the oxygen profile, due to a combination of sampling interval and removal of bad measurements. The interpolations across these gaps are nearly linear, leading to loss of curvature and

reduction in the calculated oxygen consumption rate. This strongly impacts the calculated NO_3^-/O_2 respiration ratio, which depends on the calculation of oxygen consumption rate with depth. For this reason, the calculated ratios for this zone are unreliable and we will not consider them further.

For the deeper zone, the calculated ratio is 0.0755 ± 0.0005 using Conc. BC, while using Flux BC, the calculated ratio is 0.0665 ± 0.0005 . The uncertainty due to the boundary depth between the two zones, no matter which boundary condition is chosen, is very small ($\sim 1\%$). The uncertainty due to the choice of the boundary condition (Conc. BC or Flux BC) in the deeper zone is $\sim 10\%$.

The best-fit ratio, in the one-zone model, is 0.100 ± 0.003 using the Conc. BC and 0.092 ± 0.001 using the Flux BC. The calculated ratio for the upper zone, in the two-zone model, is not considered due to large errors, and the ratio for the deeper zone is $\sim 30\%$ lower than the ratio from one-zone case.

Site U1370

The calculated NO_3^-/O_2 respiration ratio in the upper zone is 0.097 ± 0.007 . The uncertainty caused by the choice of the boundary depth between the two zones is $\sim 15\%$. For the deeper zone, the calculated ratios are 0.106 ± 0.030 using Conc. BC and 0.072 ± 0.017 using Flux BC. The relatively higher uncertainties in the deeper zone reflect a stronger impact of the boundary depth on the deeper zone than the upper zone at this site.

The ratios calculated in the upper zone, in the two-zone model, are within $\sim 10\%$ of the ratio calculated in the one-zone model (0.098 ± 0.004 using the Conc. BC and

0.090 \pm 0.002 using the Flux BC). For the deeper zone, the calculated ratios are bracketed by values from the one-zone model, although with a relatively higher uncertainty range.

In general, the uncertainties due to the boundary conditions and boundary depth between the two zones, for all the three sites, are approximately 10% to 20%. In comparison, the difference between calculated respiration ratios for the upper zone and in the one-zone model are within 10 % while the difference between the deeper zone and the one-zone model is within 30%. The greater difference in the deeper zone might be due to the greater uncertainty related to the smaller curvature in the concentration profile in the deeper sediment. With this greater uncertainty in mind, there is no clear identification of a significant change in the respiration ratio with depth.

DISCUSSION

Profile curvatures and microbial bioenergetics

In our analysis, we assume that the interstitial water chemical profiles of nitrogen and oxygen are in diffusive steady state. The characteristic time to establish steady state in a sediment column is $L^2/2D^*$, where L is the sediment column thickness and D^* is the diffusion coefficient corrected for the sediment tortuosity (McDuff and Gieskes, 1976). The time scale for both oxygen and nitrate is less than 260 thousand years (kyr) for Sites 10 and 11 and 130 kyr for Site U1370. The steady state assumption also implicitly assumes that respiration rates do not vary on this time scale and that bottom water changes in oxygen and nitrate are not the dominant cause of the observed changes in oxygen and nitrate concentrations.

The assumption of constant respiration rates on the time scale of tens to hundreds of thousand years is well justified since the sediments are millions of years old. The assumption of constant bottom-water oxygen and nitrate concentration is justified by comparison of the oxygen profiles at different sites. If past variation in bottom-water oxygen concentration is the dominant cause of the oxygen variation observed in the sediment profiles, then nearly identical variations should be observed for all the three sites. However, this is not observed. We thus rule out the possibility of relic signatures dominating the curvature of the oxygen and nitrate profiles. Additionally, the occurrence of microbial cells throughout the analyzed portions of the sediment columns (Expedition 329 Scientists, 2011a; Kallmeyer *et al.*, 2012) is consistent with microbial respiration.

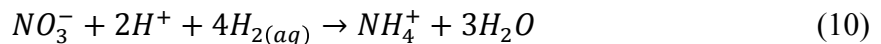
Based on our F-test results, detectable curvature in the oxygen profile exists to a depth of 14.2 m, 19.8 m and 39.8 m (41.8 m for adjusted depth) at Site 10, 11 and U1370, respectively. The corresponding ages of the sediment cores within the analysis interval at Site 10, Site 11 and Site U1370 are 10-28 Ma, 65 Ma, and 42-44 Ma, respectively. At all sites, the depth where oxygen curvature is detected, nitrate curvature is also significantly detectable. This implies that where there is oxygen consumption, there is nitrate production. In principle, curvature may result from a variation in tortuosity (McDuff and Gieskes, 1976). However, at these sites, tortuosity is nearly constant (Lado Insua, 2013). Thus, microbial aerobic respiration occurs everywhere throughout the depth intervals analyzed, and nitrogen is not depleted in the organic matter respired by sedimentary microbes. If it were, there would not be continuous nitrate production throughout this depth interval.

There are two potential sources of organic matter, detrital organic matter and subseafloor microbial biomass, supplying the nitrate production and fueling the oxygen consumption. Here we show that microbial biomass is not a significant source compared to detrital organic matter by using the cell abundance profiles and sedimentation rates. The magnitudes of the carbon flux produced by decomposing cells, at Site 10, 11 and U1370, are 10^{-20} , 10^{-21} and 10^{-22} g/cm² s, respectively, which are approximately 5 to 6 magnitudes lower than the carbon flux inferred from the oxygen flux into the interstitial water (based on the oxygen gradient at the sediment column-water boundary). Similarly, the magnitudes of the nitrogen fluxes produced by decomposing cells at each site approximate 10^{-21} g/cm² s, which is also 5 to 7 magnitudes less than total diffusive nitrogen fluxes. These comparisons indicate that

the source of the organic matter respired by sedimentary microbes is not simply decomposition of in-situ microbial cells but detrital organic matter that was deposited from the overlying ocean.

The availability of detrital reduced nitrogen compounds potentially has a large impact on microbial bioenergetics. The amino acids in sedimentary microbial biomass turn over and must be replaced to sustain a steady-state community. However, the observation that N-rich compounds are preferentially degraded suggests that the C/N ratio of the organic matter that can be respired will increase with depth until available N is depleted.

If organic nitrogen were depleted, in oxic sediment, microorganisms would have to reduce NO_3^- or fix N_2 to N (-III). Reduction of nitrate, however, is highly energetically unfavorable in oxic sediment. McCollom & Amend (2005) have investigated the energy requirement for biomass synthesis by chemolithoautotrophic microorganisms in oxic environment by the following reaction:



The Gibbs energy of this reaction is $301 \text{ KJ} \cdot (\text{mol NH}_4^+)^{-1}$ (at 25°C , 1 bar). This means that approximately $3000 \text{ J (g cell)}^{-1}$ of additional metabolic energy is required to use nitrate rather than organic nitrogen as the nitrogen source for biomass fixation.

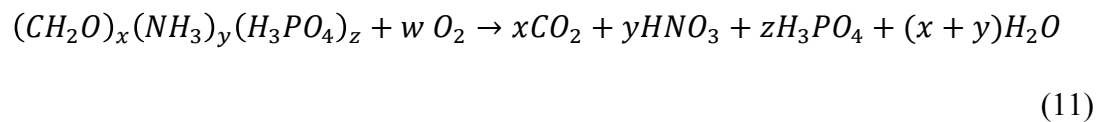
In environments with little exogenous organic matter input and limited energy, like deep seafloor sediment in the Pacific gyres, microbial metabolic energy plays an important role in governing the structure of the ecosystem. The potential for growth and reproduction of the sedimentary microorganisms depends on how efficiently they can convert the available energy into biomass, and minimize the amount of energy lost

as heat or organic by-products (McCollom & Amend, 2005). Røy *et al.* (2012) quantified aerobic microbial respiration in 86-million-year-old deep-sea sediment in the Pacific Gyre and inferred that the size of the microbial communities ultimately depends on the total available energy flux. If microbial communities need to spend a relative large amount of energy to reduce nitrate as their nitrogen source, their ecological efficiency decreases, which would result in restriction of the growth and reproduction of the microorganisms. This would strongly impact the size of microbial communities beneath the seafloor.

Our analysis demonstrates that reduced organic nitrogen is still available in organic-poor sediments that are millions of years old. Consequently, microorganisms in these sediments do not pay the energetic cost of reducing nitrate to synthesize organic matter.

Dissolved nitrate vs. dissolved oxygen

The aerobic respiration of microbes in subseafloor sediment can be expressed simply by a general equation (revised from the equation of Redfield *et al.* (1963)), assuming the C/N ratio of the organic matter is x/y :



The oxygen demand to completely oxidize the organic matter, w in equation (11), is a function of C/N ratio (x/y), and the oxidation state of carbon (ox) in the organic matter:

$$w = \left(1 - \frac{ox}{4}\right) * x + 2y \quad (12)$$

The correlation between nitrate production and oxygen consumption therefore reflects microbial aerobic respiration and the C/N stoichiometry of organic matter consumed during this process.

Dissolved oxygen is generally linearly correlated to dissolved nitrate at all three sites (Figure 5), except for a negative deviation when oxygen falls to less than 7-8 $\mu\text{mol L}^{-1}$ at Site U1370. This deviation is likely due to a diffusive flux into the basement or sedimentary denitrification, since 7-8 $\mu\text{mol L}^{-1}$ is generally thought to be the oxygen level below which denitrification occurs (Burdige, 2006). If we eliminate the data with oxygen concentrations that are below 7-8 $\mu\text{mol L}^{-1}$, in other words, we do not consider the sediment samples collected below the depth where denitrification might occur, dissolved oxygen and nitrate are linearly correlated and the slope is -0.098 ± 0.005 (95% confidence level).

This slope of the linear correlation between dissolved oxygen and nitrate is very similar to the Redfield NO_3^-/O_2 ratio in much of the ocean, 0.093 (Takahashi *et al.*, 1985) and 0.094 (Anderson & Sarmiento, 1994). Additionally, in a very short pelagic core (0.5 mbsf) from the equatorial Pacific, Grundmanis & Murray (1982) measured the dissolved NO_3^- and O_2 in interstitial water and also reported a linear correlation between dissolved oxygen and nitrate of -0.099 ± 0.015 , and the C/N ratio is 8.1 ± 2.2 (Table 2). Our data extend this result to a much greater depth (the maximum depth is about 40 mbsf at Site U1370) and much older sediments. However, the dissolved NO_3^-/O_2 ratio from our samples is indistinguishable with their results.

Diffusion-Reaction model analysis

The one-zone model

We estimate the best-fit NO_3^-/O_2 respiration ratio based on the curvature of oxygen and nitrate profiles. The calculated ratios are given in Table 2. Based on the assumption of steady state, the calculated NO_3^-/O_2 respiration ratios and the average oxidation state of carbon, we determined the C/N ratio of the organic matter respired during the aerobic respiration. We use -0.7 to 0 for the carbon oxidation state range (Redfield *et al.*, 1963; Hedges *et al.*, 2002). The calculated C/N ratios at all of the three sites, are within the range of 8.0 to 9.2 for carbon with oxidation state of 0, and 6.8 to 7.9 for carbon with oxidation state of -0.7.

The best-fit NO_3^-/O_2 respiration ratios at the three sites are very similar to each other and cannot be distinguished, within the uncertainty of 10%, no matter which boundary condition is used for the model. The modeled NO_3^-/O_2 respiration ratios are very close to the linear slope, -0.098, of the dissolved N/ O_2 correlation (Figure 5).

Moreover, these calculated NO_3^-/O_2 respiration ratios and the C/N ratio from our model analysis are also very similar to the Redfield C/ NO_3^-/O_2 ratio measured in the water column in the entire ocean, which is 140:16:172, i.e. 0.093 for N/ O_2 ratio and 8.75 for C/N ratio (Takahashi *et al.*, 1985), and 117:16:170, i.e. 0.094 for N/ O_2 ratio and 7.3 for C/N ratio (Anderson & Sarmiento, 1994).

The two-zone model

Within the uncertainties of the model due to the choice of boundary conditions and boundary depths between the two zones, there is no clear indication that the

respiration ratio varies with depth. The uncertainties due to the boundary conditions and boundary depth between the two zones, for all the three sites, are ~ 10% to 20%. Within this range of uncertainty, we are not able to determine whether there is real variation of the respiration with depth or it is only due to the assumptions of the model settings. As mentioned above, the variation of the respiration ratio for the upper zone is within 10% and for the deeper zone is within 30%. These variations are not significant since they are almost at the same magnitude of the uncertainty due to model assumptions.

If the NO_3^-/O_2 respiration ratio is constant through the analyzed depth interval, the chemical stoichiometry of organic matter consumed by microbes beneath the seafloor, at these three sampled sites in the Pacific gyres, is similar to the C/N ratio of organic matter in the modern ocean (the Redfield C/N ratio). We consider two possible explanations for this nearly constant respiration ratio:

- 1) The chemical composition of organic matter consumed is similar to that in the modern ocean and has not changed for ~ 65 million years. There is no fractionation of C/N ratio during respiration.

- 2) Sedimentary microbes respire organic matter according to the Redfield ratio, even if the chemical composition of the bulk sedimentary organic matter has a different C/N ratio due to either change with time in the oceanic Redfield Ratio or fractionation in the water column or during sedimentation.

The first explanation, however, is inconsistent with the observation of preferential N degradation. The C/N ratio of the organic matter in the water column and sediment are observed to increase with depth (Arrhenius, 1953; Bishop *et al.*,

1977; Knauer *et al.*, 1979). In contrast, the second explanation is more consistent. Even though the C/N ratio of the bulk sedimentary organic matter may differ from the Redfield ratio, at these sites, microbes only respire organic matter with the Redfield ratio. The respiration of organic matter with this nearly constant ratio may be controlled by the nutrient requirement of microbial communities and selection pressure to maximize ecological efficiency.

SUMMARY

In summary, we used a diffusion-reaction model to analyze the NO_3^-/O_2 respiration ratio from dissolved oxygen and nitrate in the interstitial water of subseafloor sediment samples collected in the Pacific gyres. Based on the curvature of the concentration profiles, we determined that nitrogen is not depleted in the respired sedimentary organic matter, up to ~ 65 million years old, during aerobic respiration. This implies that microbes do not expend additional energy to reduce nitrate or fix dinitrogen, which eases the stress of energy limitation for microbial communities in the deep subseafloor sediment and maximizes their ecological efficiency. Oxygen and nitrate profiles are well explained by the one-zone model with a constant NO_3^-/O_2 respiration ratio with depth. Comparison of the calculated respiration ratios from the one-zone model and the two-zone model reveals that, within the model uncertainties, there is no clear indication that the respiration ratio varies with sediment depth. The respiration ratios are indistinguishable from the water column $\text{C}/\text{NO}_3^-/\text{O}_2$ Redfield ratio. This implies that subseafloor aerobic microbes utilize organic carbon and nitrogen with a C/N ratio that is constant and indistinguishable from the Redfield ratio, independent of the C/N ratio of the bulk organic matter.

LIST OF REFERENCES

- Anderson, L. A., & Sarmiento, J. L. (1994). Redfield ratios of remineralization determined by nutrient data analysis. *Global Biogeochemical Cycles*, 8 (1), 65-80.
- Arrhenius, G. (1953). Sediment cores from the East Pacific. *GFF*, 75(1), 115-118.
- Barreto, L. A., Milliman J. D., Amaral, C. A. B. and Francisconi O., (1975). Northern Brazil. In Upper Continental Margin Sedimentation off Brazil (editors J. D. Milliman and C. P. Summerhayes) *Contributions to Sedimentology. Vol. 4. pp 11-43 E. Schweizerbart.*
- Becker, T.W., Conrad, C.P., Buffett, B. and Müller, R.D., 2009, Past and present seafloor age distributions and the temporal evolution of plate tectonic heat transport, *Earth and Planetary Science Letters*, 278, 233-242
- Bishop, Edmond, Ketten, Bacon and Silker, (1977). The chemistry, biology and vertical flux of particulate matter from the upper 400 m of the equatorial Atlantic ocean. *Deep-Sea Res.* 24, 511-548
- Burdige, D. J. (2006). *Geochemistry of marine sediments* (Vol. 398). Princeton: Princeton University Press.
- Da Rocha, J., Milliman J. D., Santana C. I. and Vicalvi M. A. (1975). Southern Brazil. In Upper Continental Margin Sedimentation off Brazil (editors J. D. Milliman and C. P. Summerhayes) *Contributions to Sedimentology. Vol. 4. pp 117-150 E. Schweizerbart.*
- Devol, A. H. (1978). Bacterial oxygen uptake kinetics as related to biological processes in oxygen deficient zones of the oceans. *Deep Sea Research*, 25 (2), 137-146.
- D'Hondt, S., Jørgensen, B. B., Miller, D. J., Batzke, A., Blake, R., Cragg, B. A., & Acosta, J. L. S. (2004). Distributions of microbial activities in deep seafloor sediments. *Science*, 306 (5705), 2216-2221.

Expedition 329 Scientists, 2011a. Site U1370. *In* D'Hondt, S., Inagaki, F., Alvarez Zarikian, C.A., and the Expedition 329 Scientists, *Proc. IODP*, 329: Tokyo (Integrated Ocean Drilling Program Management International, Inc.).

doi:10.2204/iodp.proc.329.108.2011

Expedition 329 Scientists, 2011b. Methods. *In* D'Hondt, S., Inagaki, F., Alvarez Zarikian, C.A., and the Expedition 329 Scientists, *Proc. IODP*, 329: Tokyo (Integrated Ocean Drilling Program Management International,

Inc.). **doi:10.2204/iodp.proc.329.102.2011**

Gradstein, F.M., Ogg, J.G., and Smith, A.G. (Eds.), (2004). *A Geologic Time Scale 2004*: Cambridge (Cambridge Univ. Press).

Gribsholt, B., & Kristensen, E. (2002). Impact of sampling methods on sulfate reduction rates and dissolved organic carbon (DOC) concentrations in vegetated salt marsh sediments. *Wetlands Ecology and Management*, 10(5), 371-379.

Grundmanis, V., & Murray, J. W. (1982). Aerobic respiration in pelagic marine sediments. *Geochimica et cosmochimica acta*, 46 (6), 1101-1120.

Hedges, J. I., Baldock, J. A., Gelinas, Y., Lee, C., Peterson, M. L., & Wakeham, S. G. (2002). The biochemical and elemental compositions of marine plankton: A NMR perspective. *Marine Chemistry*, 78 (1), 47-63.

Honjo, S. (1980). Material fluxes and modes of sedimentation in the mesopelagic and bathypelagic zones. *J. mar. Res.*, 38 (1), 53-97.

Kallmeyer, J., Pockalny, R., Adhikari, R. R., Smith, D. C., & D'Hondt, S. (2012). Global distribution of microbial abundance and biomass in subseafloor sediment. *Proceedings of the National Academy of Sciences*, 109(40), 16213-16216.

Knauer, Martin and Bruland, (1979). Fluxes of particulate carbon , nitrogen and phosphorus in the upper water column of the north-east Pacific. *Deep-Sea Res.* 26A, 97-108

Kyte, F. T., & Wasson, J. T. (1986). Accretion rate of extraterrestrial matter: Iridium deposited 33 to 67 million years ago. *Science*, 232(4755), 1225-1229.

Lado Insua, Tania, "Physical Properties of Marine Sediments and their Application Toward Climate Change Studies" (2013). Open Access Dissertations. Paper 47. http://digitalcommons.uri.edu/oa_diss/47

Larson, R.L., Pockalny, R.A., Viso, R.F., Erba, E., Abrams, L.J., Luyendyk, B.P., Stock, J.M., and Clayton, R.W. (2002). Mid-Cretaceous tectonic evolution of the Tongareva triple junction in the southwestern Pacific Basin. *Geology*, 30(1):67–70.

McCollom, T. M., & Amend, J. P. (2005). A thermodynamic assessment of energy requirements for biomass synthesis by chemolithoautotrophic micro-organisms in oxic and anoxic environments. *Geobiology*, 3 (2), 135-144.

McDuff, R. E., & Gieskes, J. M. (1976). Calcium and magnesium profiles in DSDP interstitial waters: Diffusion or reaction?. *Earth and Planetary Science Letters*, 33(1), 1-10.

Murray, J. W., & Kuivila, K. M. (1990). Organic matter diagenesis in the northeast Pacific: transition from aerobic red clay to suboxic hemipelagic sediments. *Deep Sea Research Part A. Oceanographic Research Papers*, 37 (1), 59-80.

Parkes, R. J., Cragg, B. A., Wellsbury, P., (2000). Recent studies on bacterial populations and processes in subseafloor sediments: a review. *Hydrogeol. J.*, 8(1):11–28.

Redfield, A. C., (1934). On the proportions of organic derivatives in sea water and their relation to the composition of plankton, in James Johnson Memorial Volume, pp. 177-192, Liverpool, U. K.

Redfield, A. C., B. H. Ketchum, and F. A. Richards, (1963). The influence of organisms on the composition of sea water, in *The Sea*, vol. 2, edited by M. N. Hill, pp. 26-77, Interscience, New York

Røy, H., Kallmeyer, J., Adhikari, R. R., Pockalny, R., Jørgensen, B. B., & D'Hondt, S. (2012). Aerobic microbial respiration in 86-million-year-old deep-sea red clay. *Science*, 336(6083), 922-925.

Schrump, H. N., Spivack, A. J., Kastner, M., & D'Hondt, S. (2009). Sulfate-reducing ammonium oxidation: a thermodynamically feasible metabolic pathway in subseafloor sediment. *Geology*, 37(10), 939-942.

Schulz, H. D., & Zabel, M. (Eds.). (2006). *Marine geochemistry*. Springer.

Takahashi, T., Broecker, W. S., & Langer, S. (1985). Redfield ratio based on chemical data from isopycnal surfaces. *Journal of Geophysical Research: Oceans (1978–2012)*, 90(C4), 6907-6924.

Wang, G., Spivack, A. J., Rutherford, S., Manor, U., & D'Hondt, S. (2008). Quantification of co-occurring reaction rates in deep subseafloor sediments. *Geochimica et Cosmochimica Acta*, 72(14), 3479-3488.

WOCE Atlas Volume 2: Pacific Ocean.

http://www-pord.ucsd.edu/whp_atlas/pacific_index.html, Nov. 2013

FIGURES

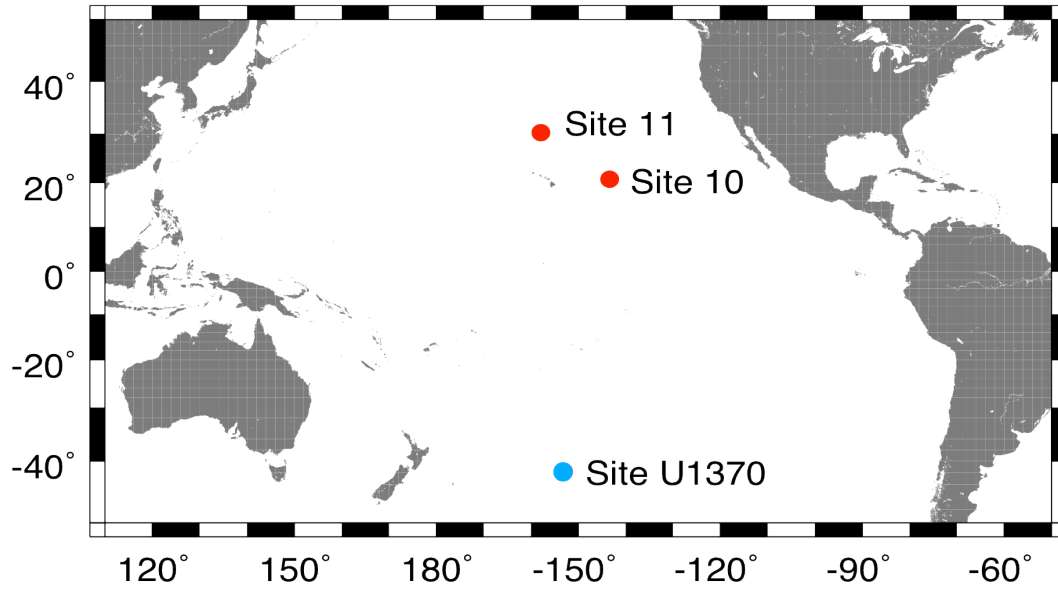


Figure 1 Location of Knorr Site 10 and Site 11 in the North Pacific Gyre and IODP Site U1370 in the South Pacific Gyre.

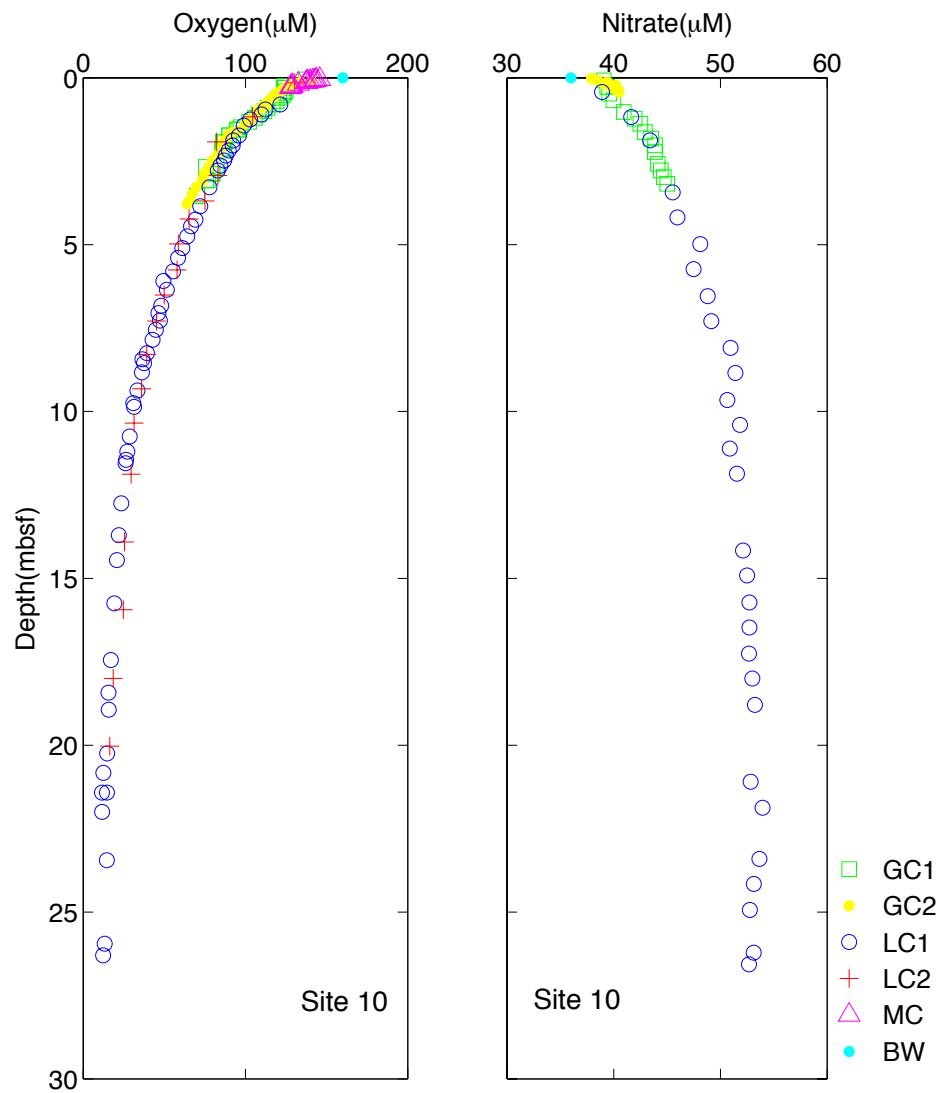


Figure 2.1 Dissolved oxygen and nitrate profiles in the interstitial water collected from multiple sediment cores at Site 10. The cyan dot at the sediment surface (BW) indicates the concentration of bottom water, which is the value from WOCE Atlas Pacific Volume 2.

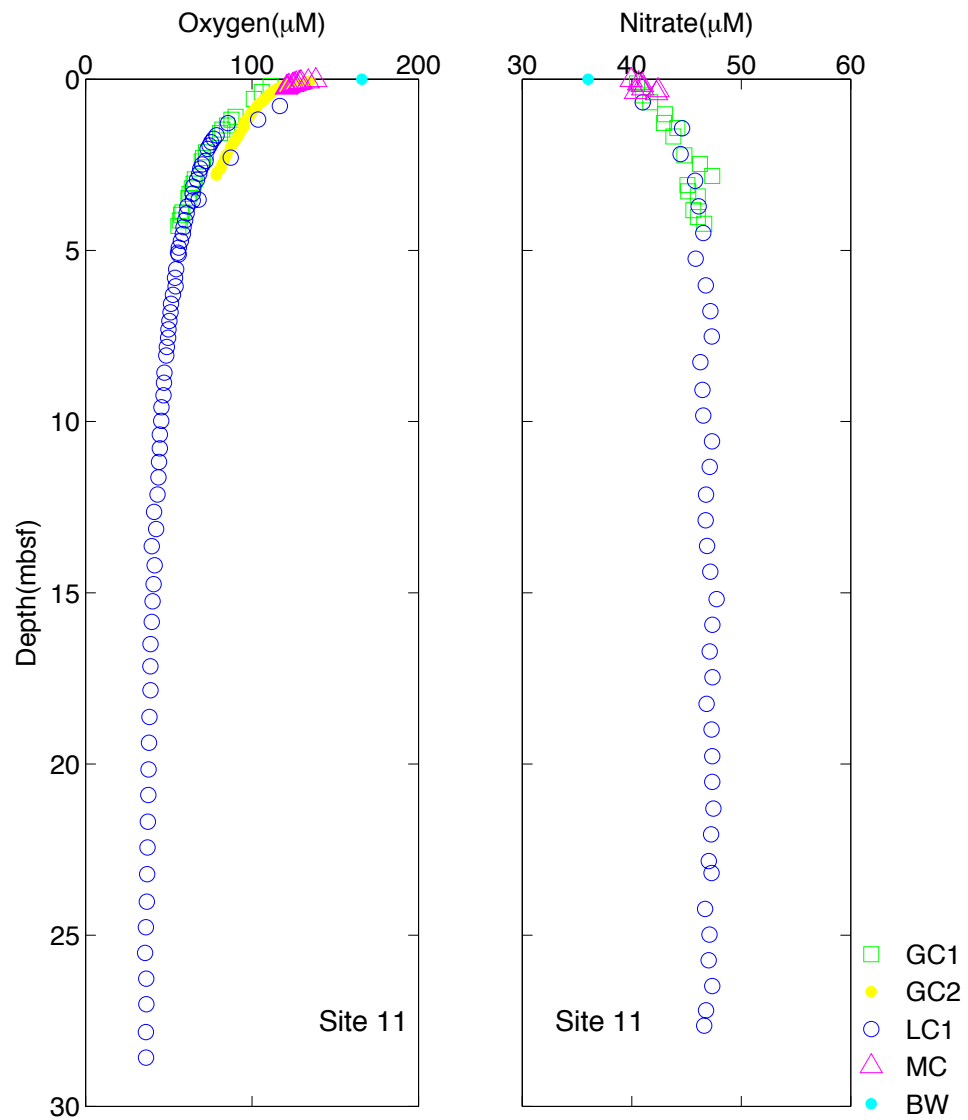


Figure 2.2 Dissolved oxygen and nitrate profiles in the interstitial water collected from multiple sediment cores at Site 11.

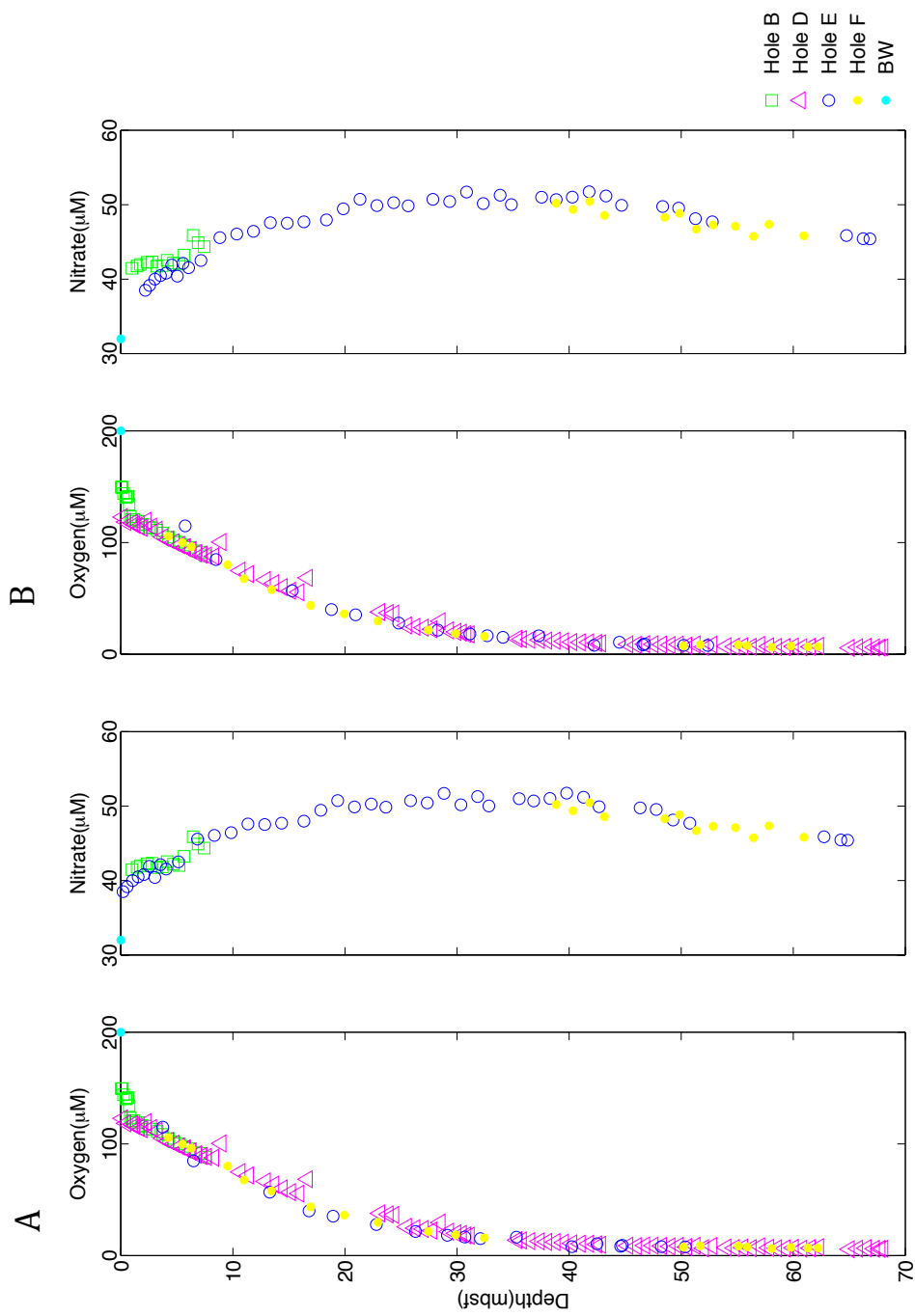


Figure 2.3 Dissolved oxygen and nitrate profiles in the interstitial water collected from multiple sediment cores at Site U1370. The oxygen and nitrate profiles of Hole E are presented in measured depth (A) and adapted depth (B), which moves the whole measured profiles of oxygen and nitrate of Hole E down about 2 meters.

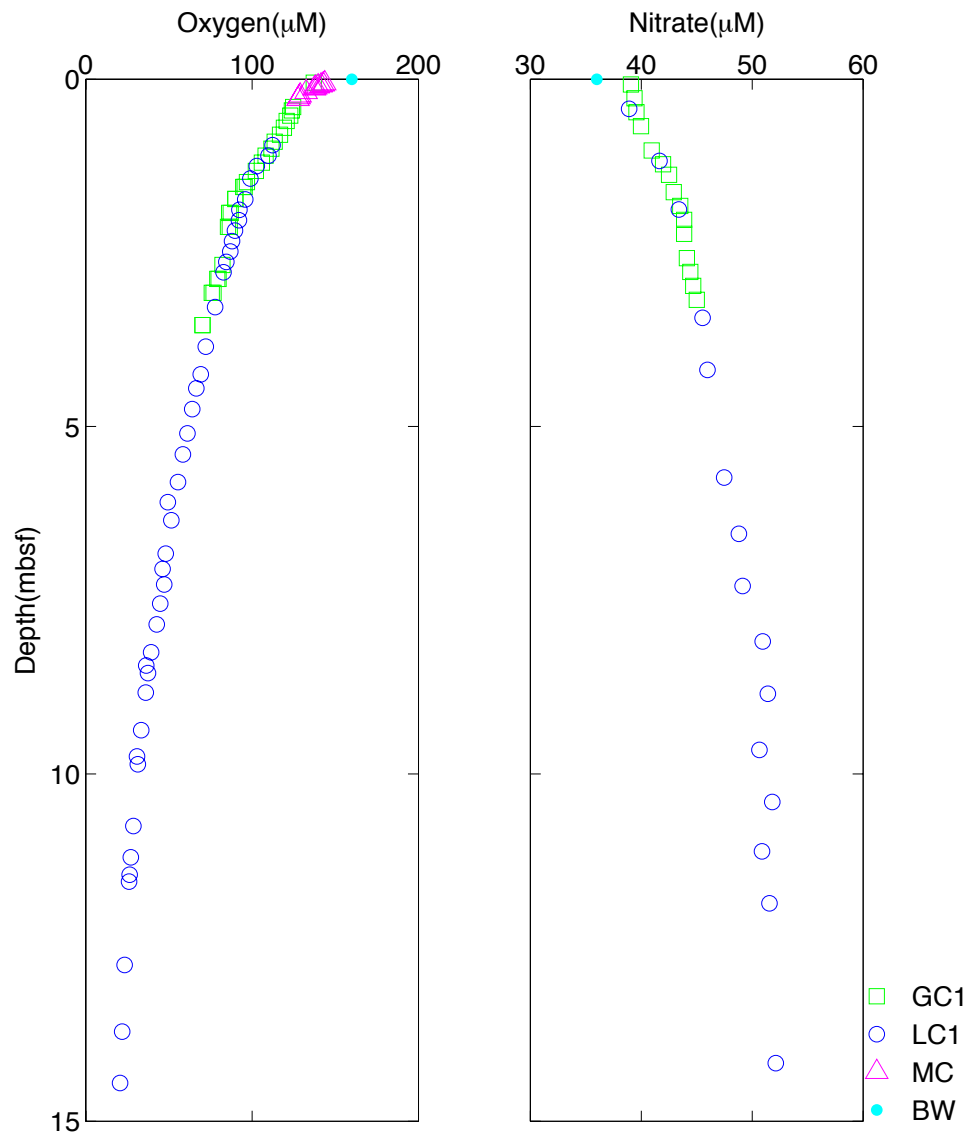


Figure 3.1 Dissolved oxygen and nitrate profiles of selected sediment cores at Site 10. The depth is limited to the 15 meters below seafloor to insure the existence of obvious curvature in both oxygen and nitrate profiles. These data are used for model analysis for this site.

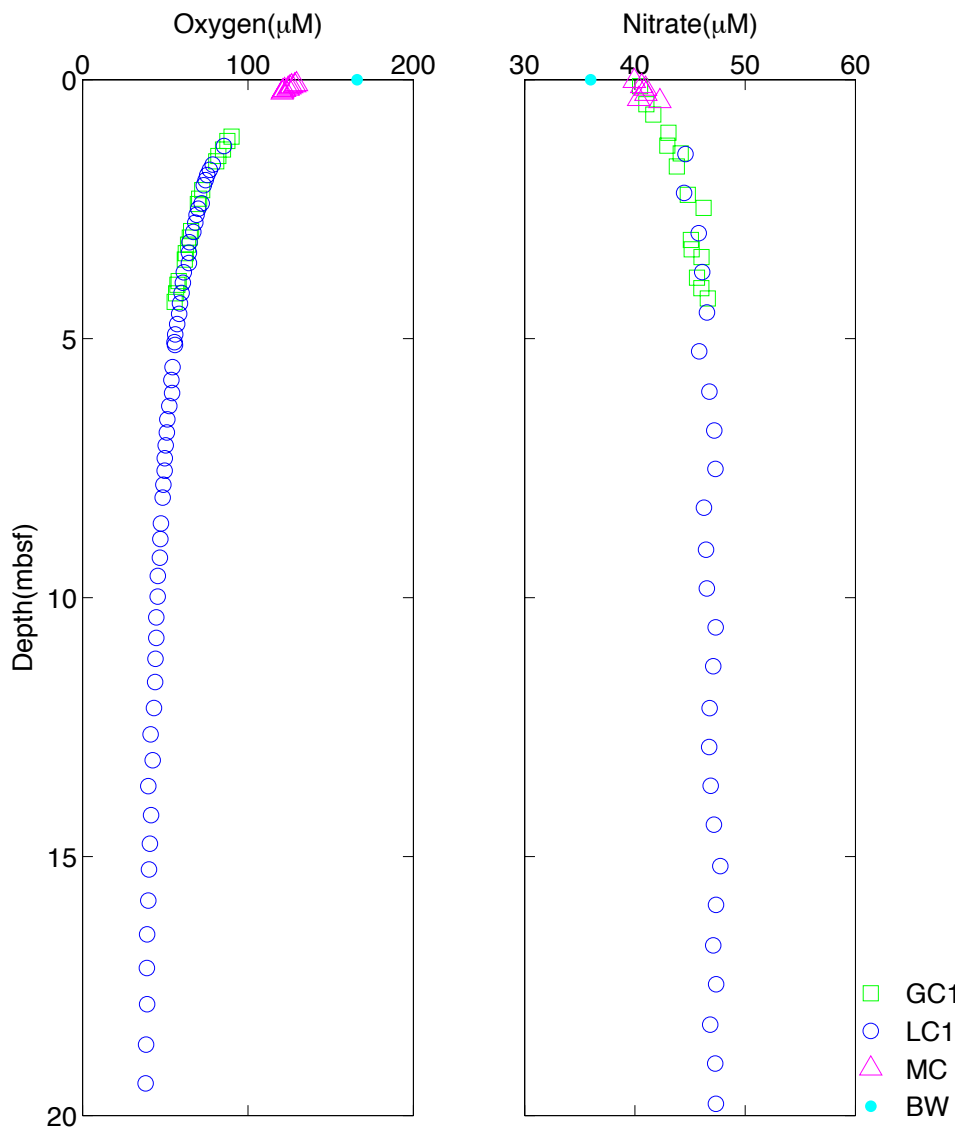


Figure 3.2 Dissolved oxygen and nitrate profiles of selected sediment cores at Site 11. The depth is limited to the 20 meters below seafloor to insure the existence of obvious curvature in both oxygen and nitrate profiles. These data are used for model analysis for this site.

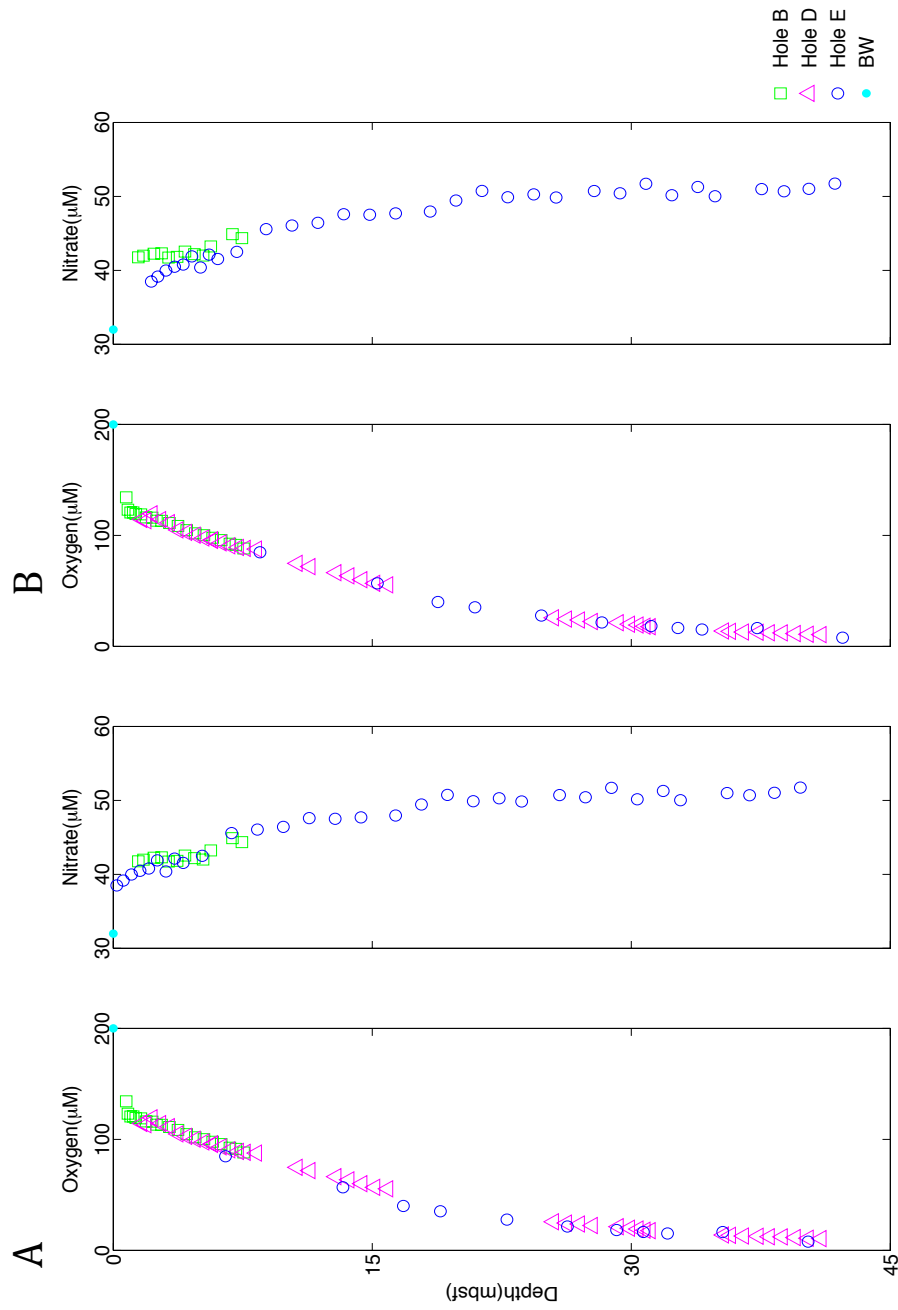


Figure 3.3 Dissolved oxygen and nitrate profiles of selected sediment cores at Site U1370. The depth is limited to the 40 meters below seafloor for measured depth (A) and 42 meters below seafloor for adapted depth (B). These data are used for model analysis for this site.

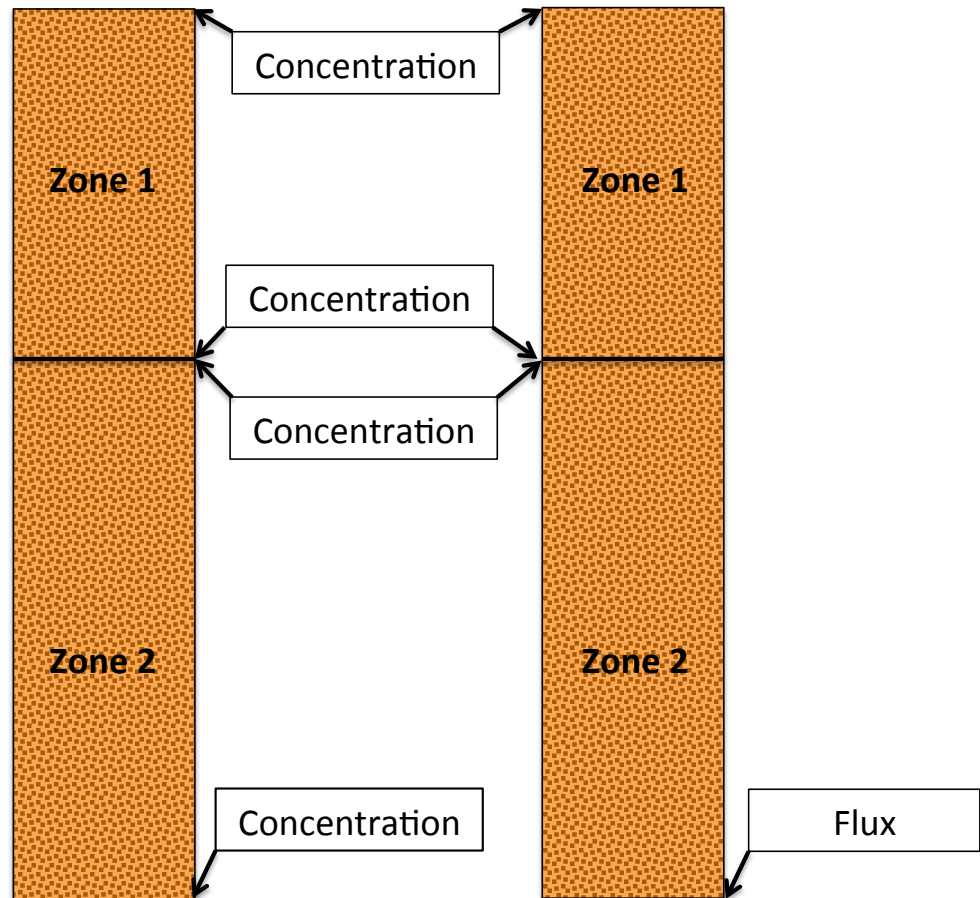


Figure 4 The diagram of the boundary conditions for two-zone case. Only Conc. BC is used for the upper zone in both cases. For the deeper zone, both Conc. BC and Flux BC are used.

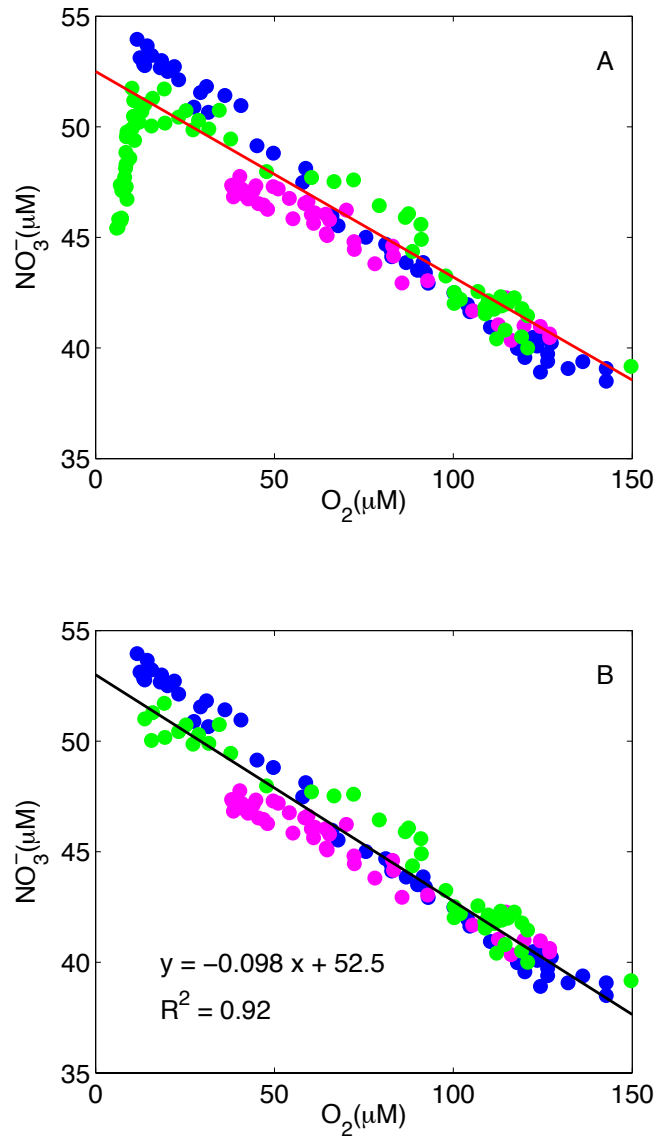


Figure 5 The plot of dissolved nitrate versus dissolved oxygen in interstitial water from all sites (Site 10: magenta; Site 11: blue; Site U1370: green). A: all data from Site U1370 are included and the red line indicates the Redfield ratio from Anderson & Sarmiento, 1994. B: only the data with oxygen concentration higher than 7-8 $\mu\text{mol L}^{-1}$ are included and the solid line is the slope of the linear regression of all data.

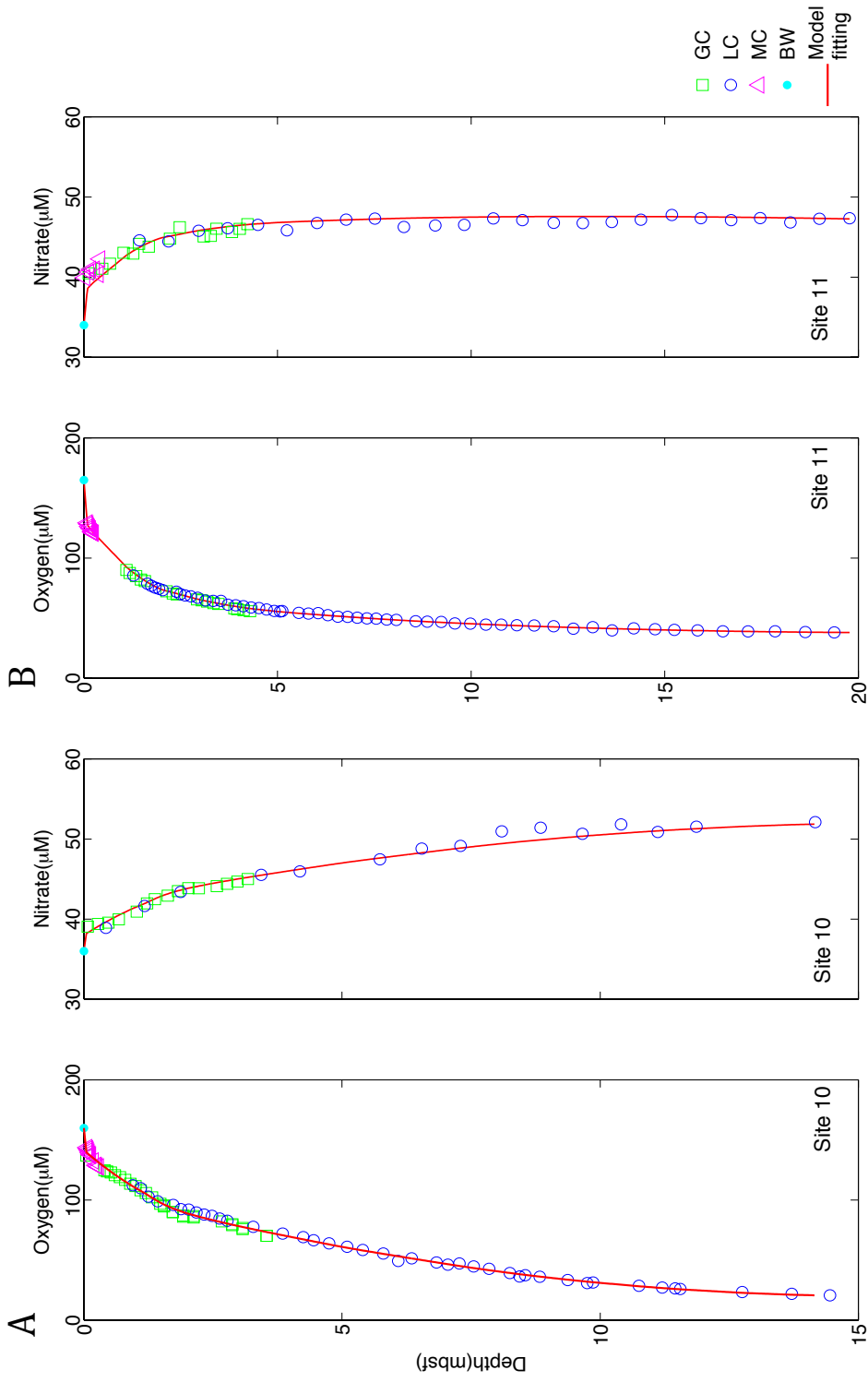


Figure 6.1 The best-fit curves (red line) for oxygen and nitrate profiles at Site 10 (A) and Site 11 (B) in the one-zone model, using Conc. BC.

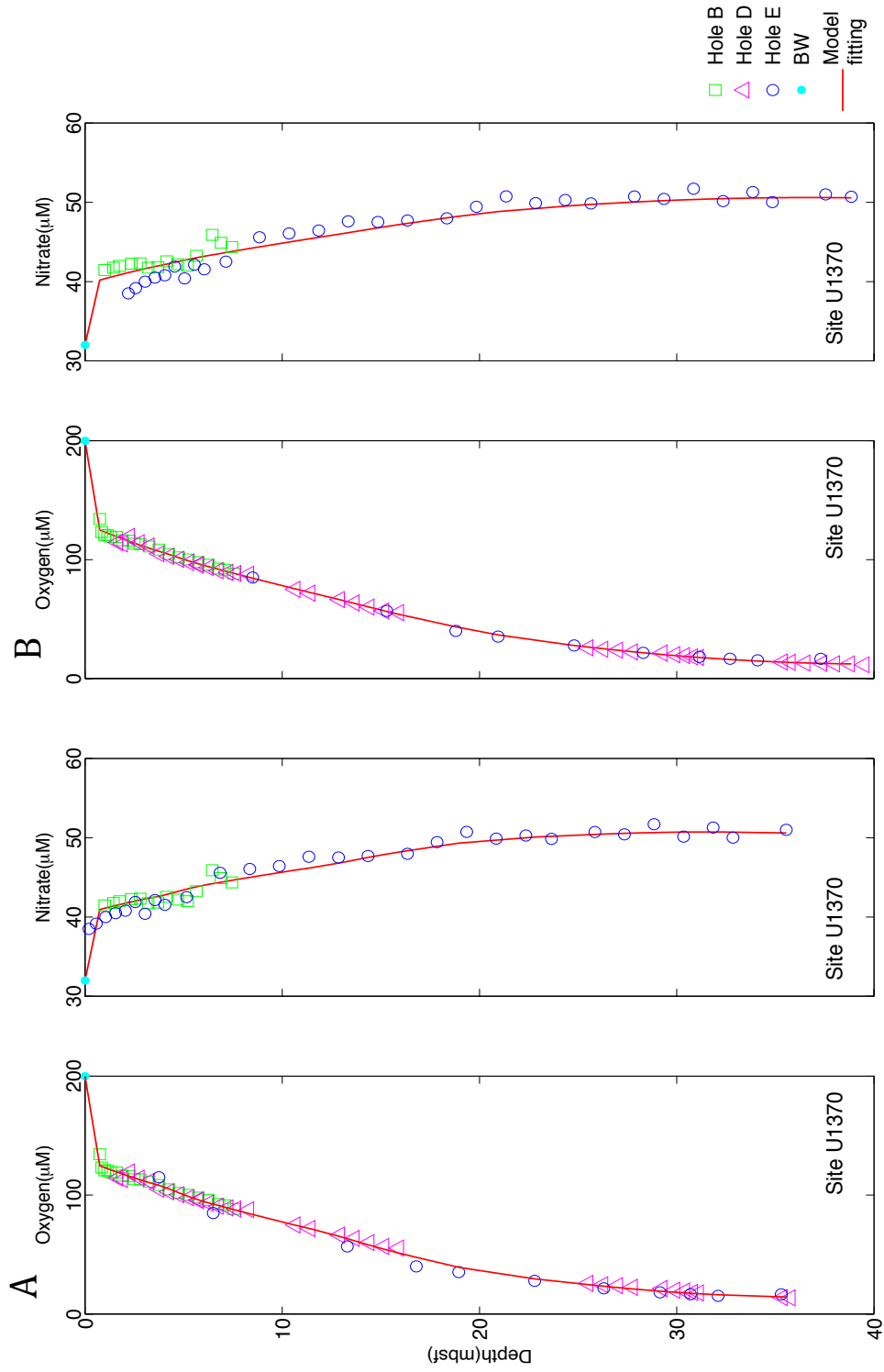


Figure 6.2 The best-fit curves (red line) for oxygen and nitrate profiles at Site U1370 in the one-zone model. The left two plots (A) use measured depth of Hole E and the right two plots (B) use adjusted depth for Hole E. Conc. BC is used.

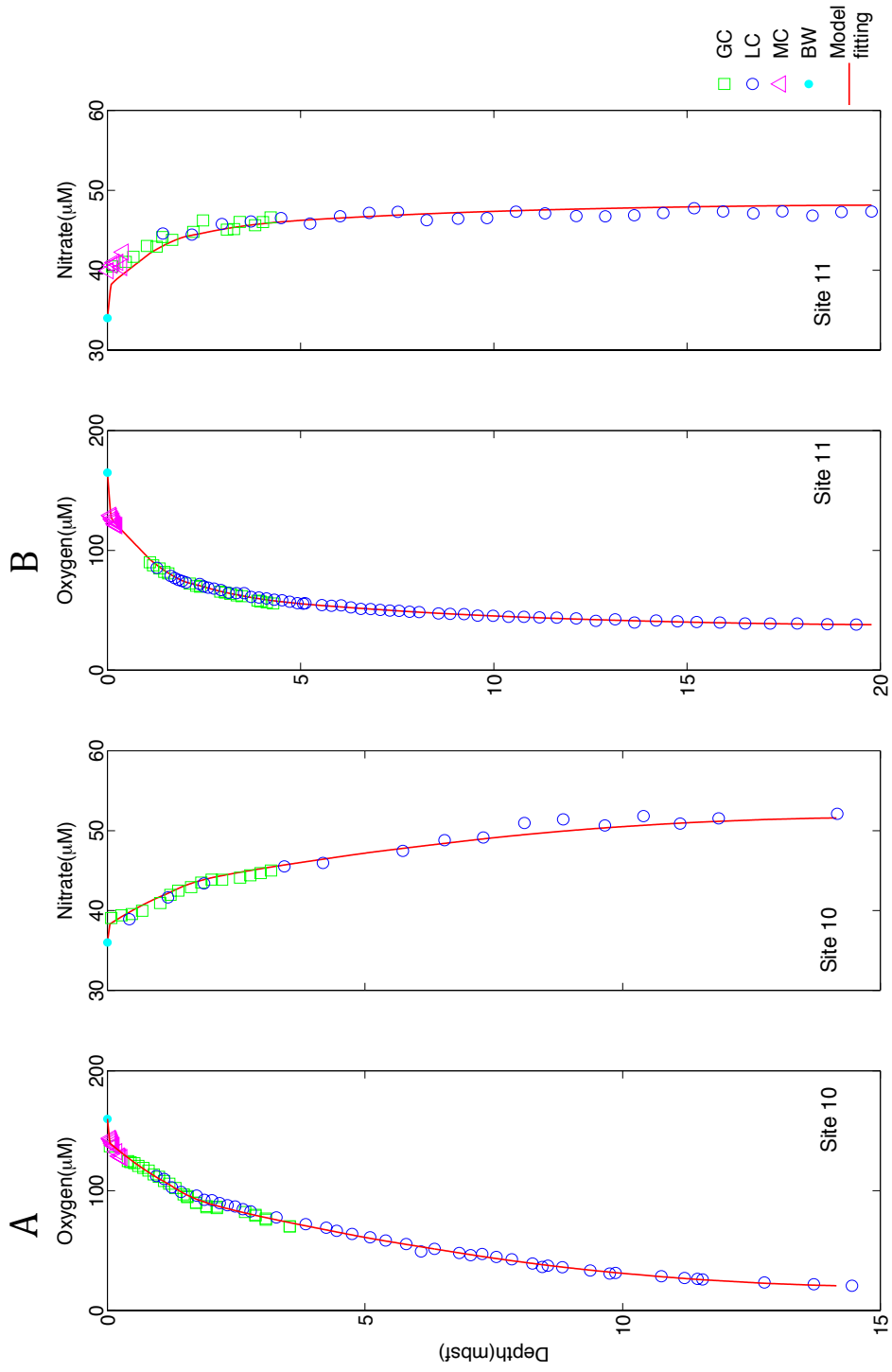


Figure 7.1 The best-fit curves (red line) for oxygen and nitrate profiles at Site 10 (A) and Site 11 (B) in the one-zone model, using Flux BC.

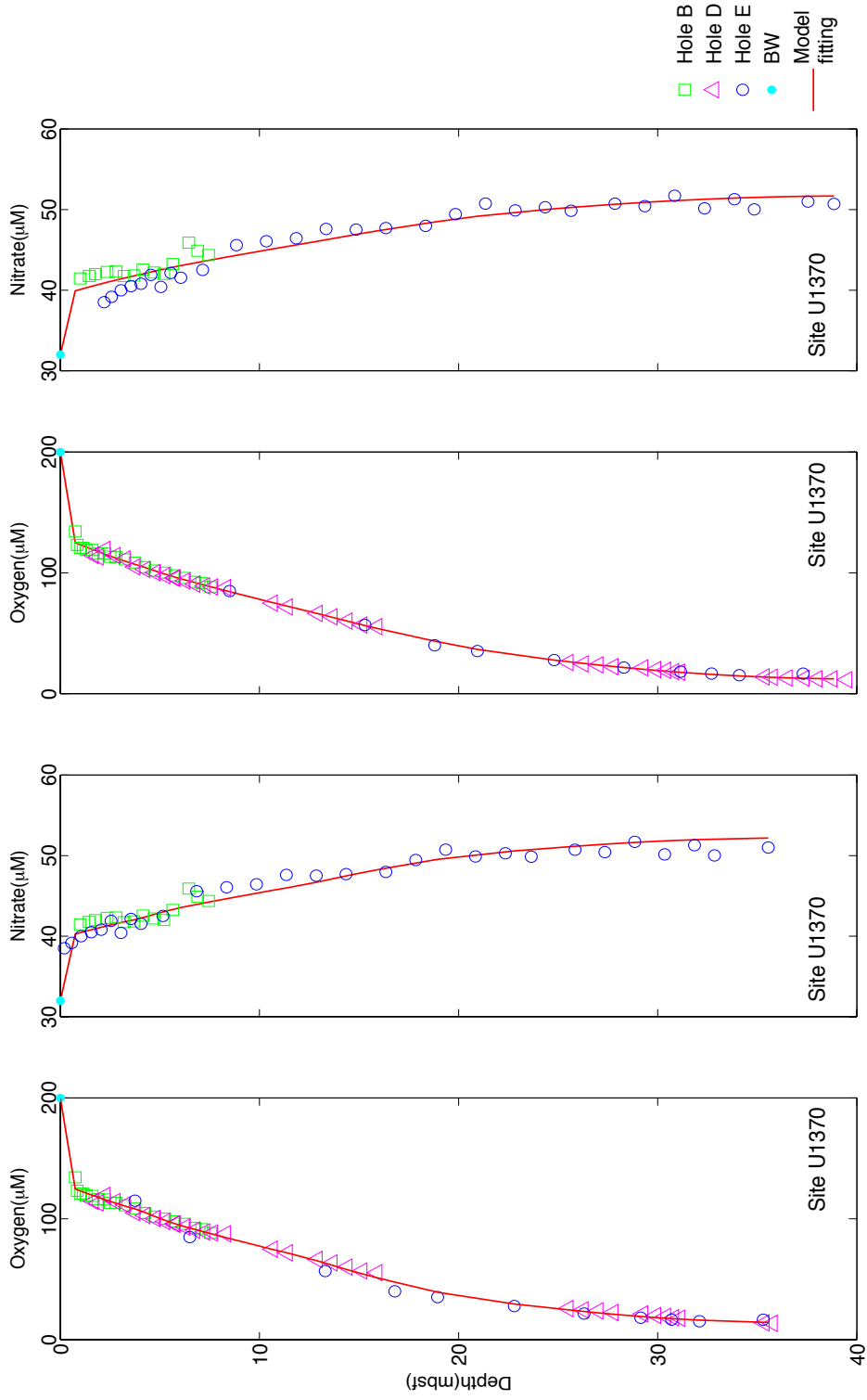


Figure 7.2 The best-fit curves (red line) for oxygen and nitrate profiles at Site U1370 in the one-zone model. The left two plots

(A) use measured depth of Hole E and the right two plots (B) use adjusted depth for Hole E. Flux BC is used.

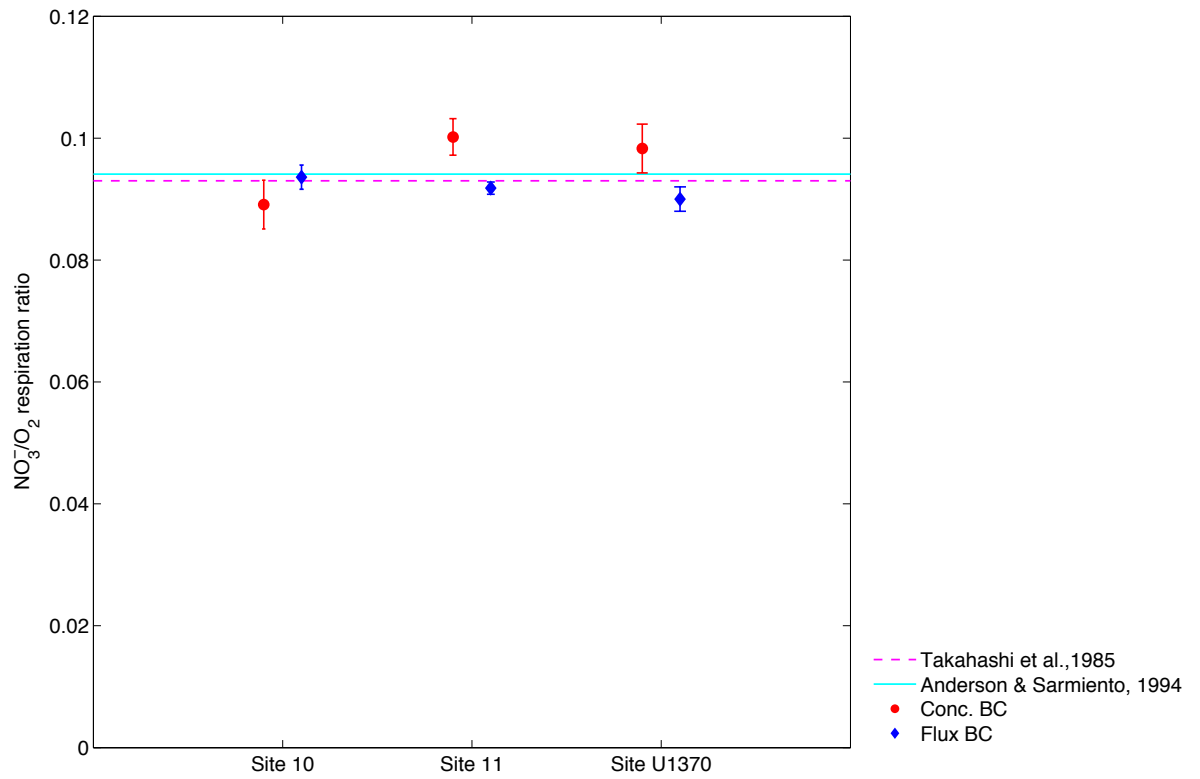


Figure 8 The best-fit NO_3^-/O_2 respiration ratios determined by model analysis at each site from the one-zone model. The magenta dash line is the NO_3^-/O_2 Redfield ratio evaluated by Takahashi *et al.*, (1985). The cyan solid line represents the NO_3^-/O_2 Redfield ratio measured by Anderson & Sarmiento (1994).

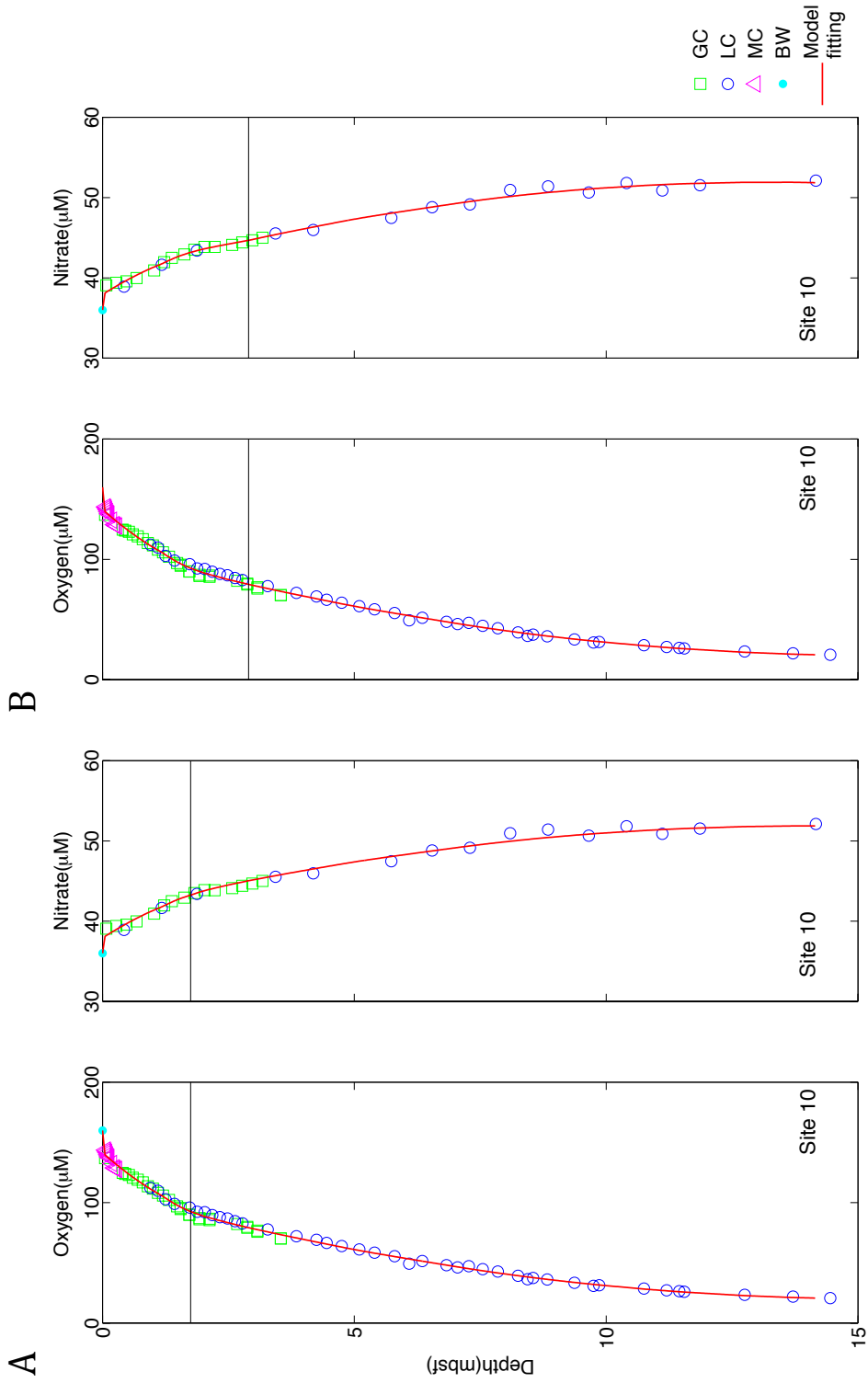


Figure 9.1 The best-fit oxygen and nitrate curves from the two-zone model at Site 10. The solid horizontal lines indicate the depth where the sediment column is separated. Conc. BC is used for the deeper zone.

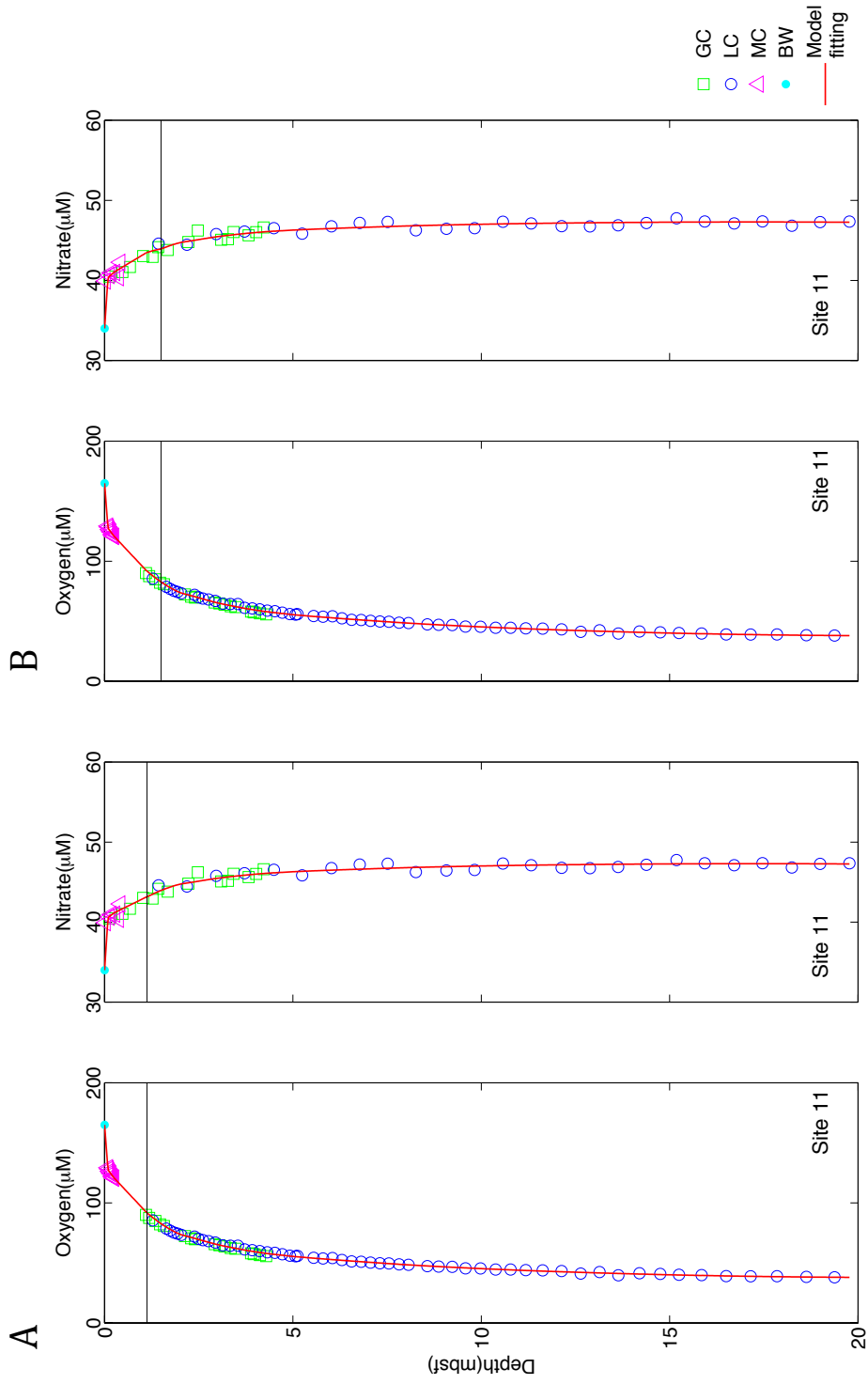


Figure 9.2 The best-fit oxygen and nitrate curves from the two-zone model at Site 11. The solid horizontal lines indicate the depth where the sediment column is separated. Conc. BC is used for the deeper zone.

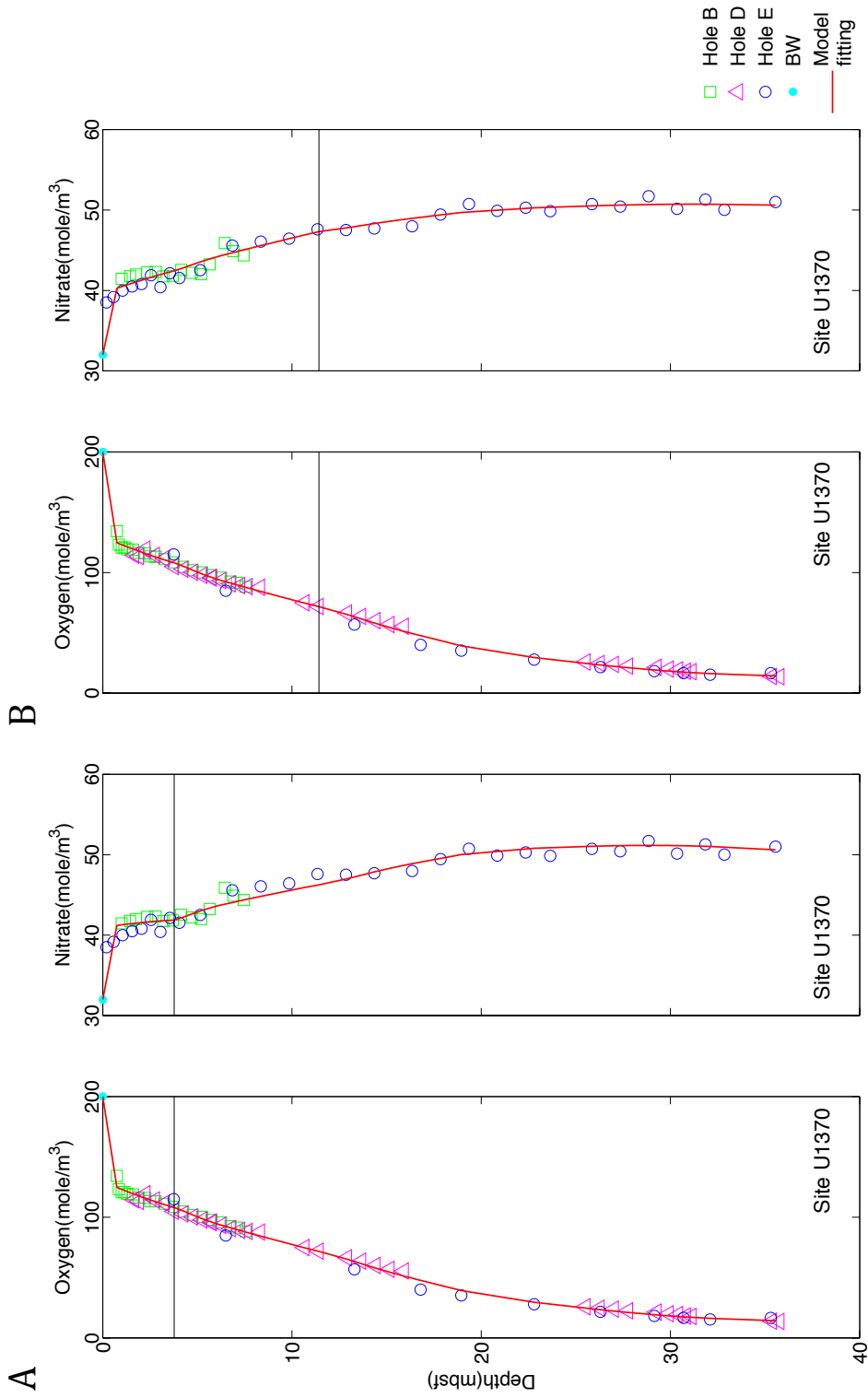


Figure 9.3 The best-fit oxygen and nitrate curves from the two-zone model at Site U1370. Measured depth of Hole E is used. The solid horizontal lines indicate the depth where the sediment column is separated. Conc. BC is used for the deeper zone.

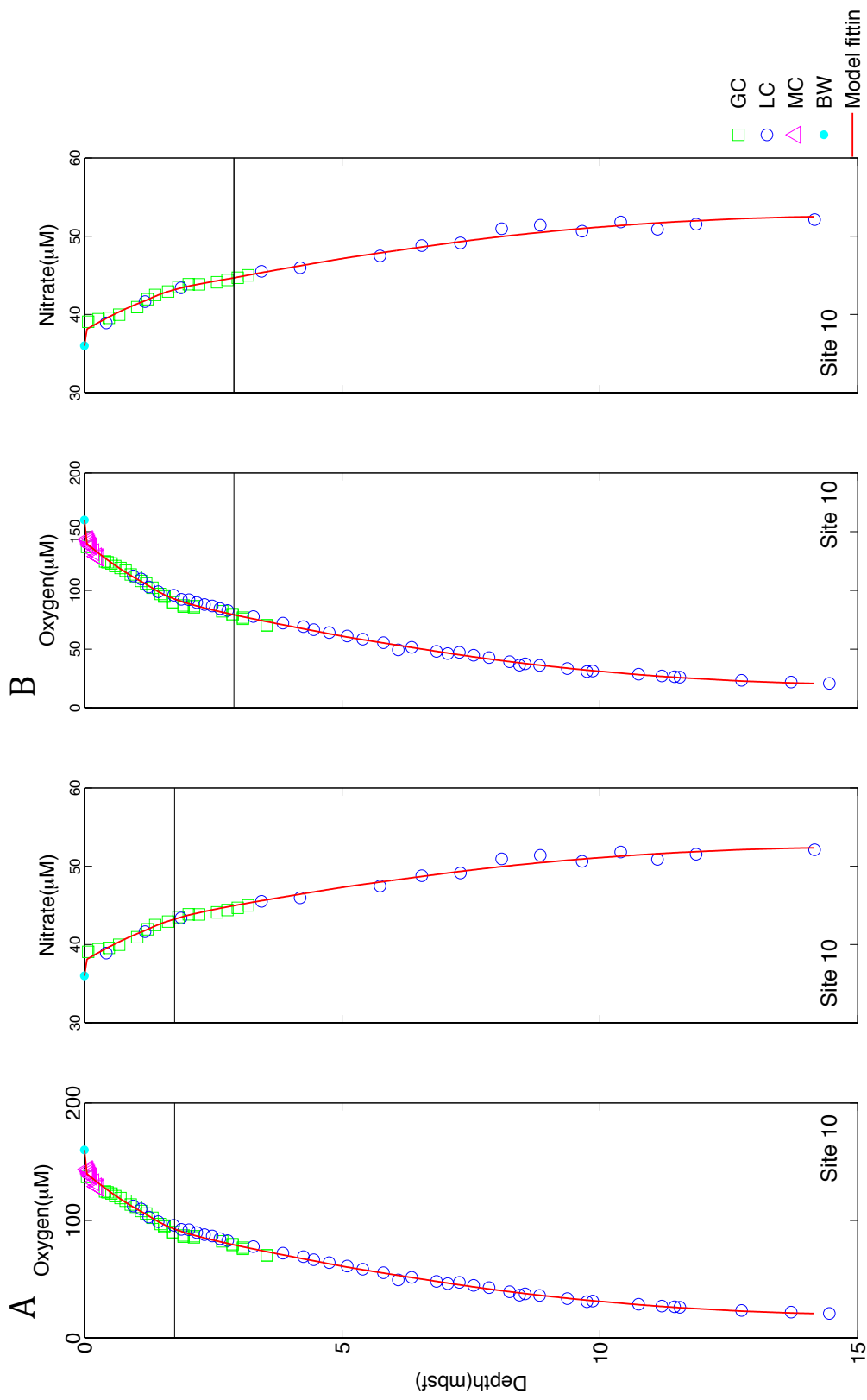


Figure 10.1 The best-fit oxygen and nitrate curves from the two-zone model at Site 10. The solid horizontal lines indicate the depth where the sediment column is separated. Flux BC is used for the deeper zone.

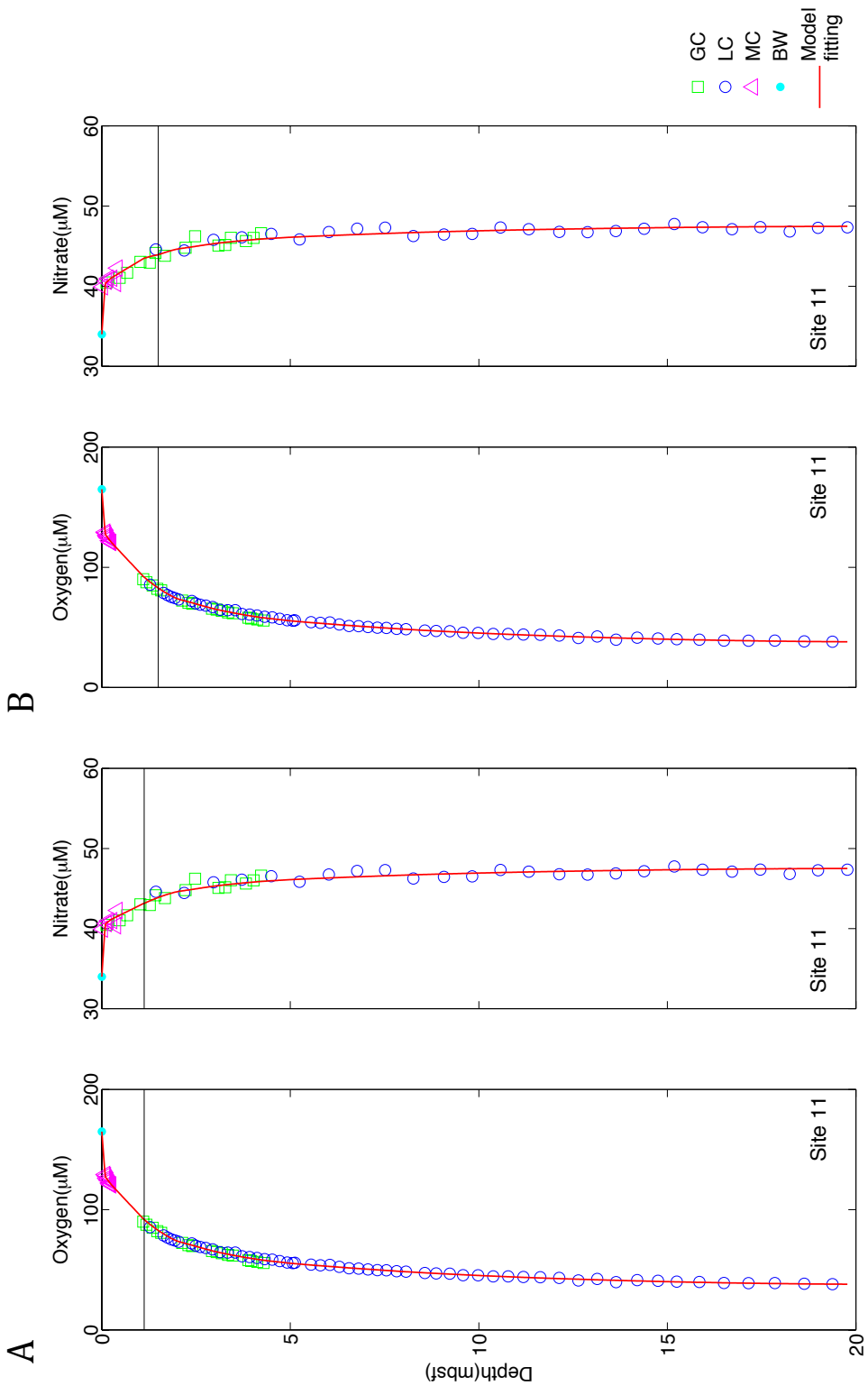


Figure 10.2 The best-fit oxygen and nitrate curves from the two-zone model at Site 11. The solid horizontal lines indicate the depth where the sediment column is separated. Flux BC is used for the deeper zone.

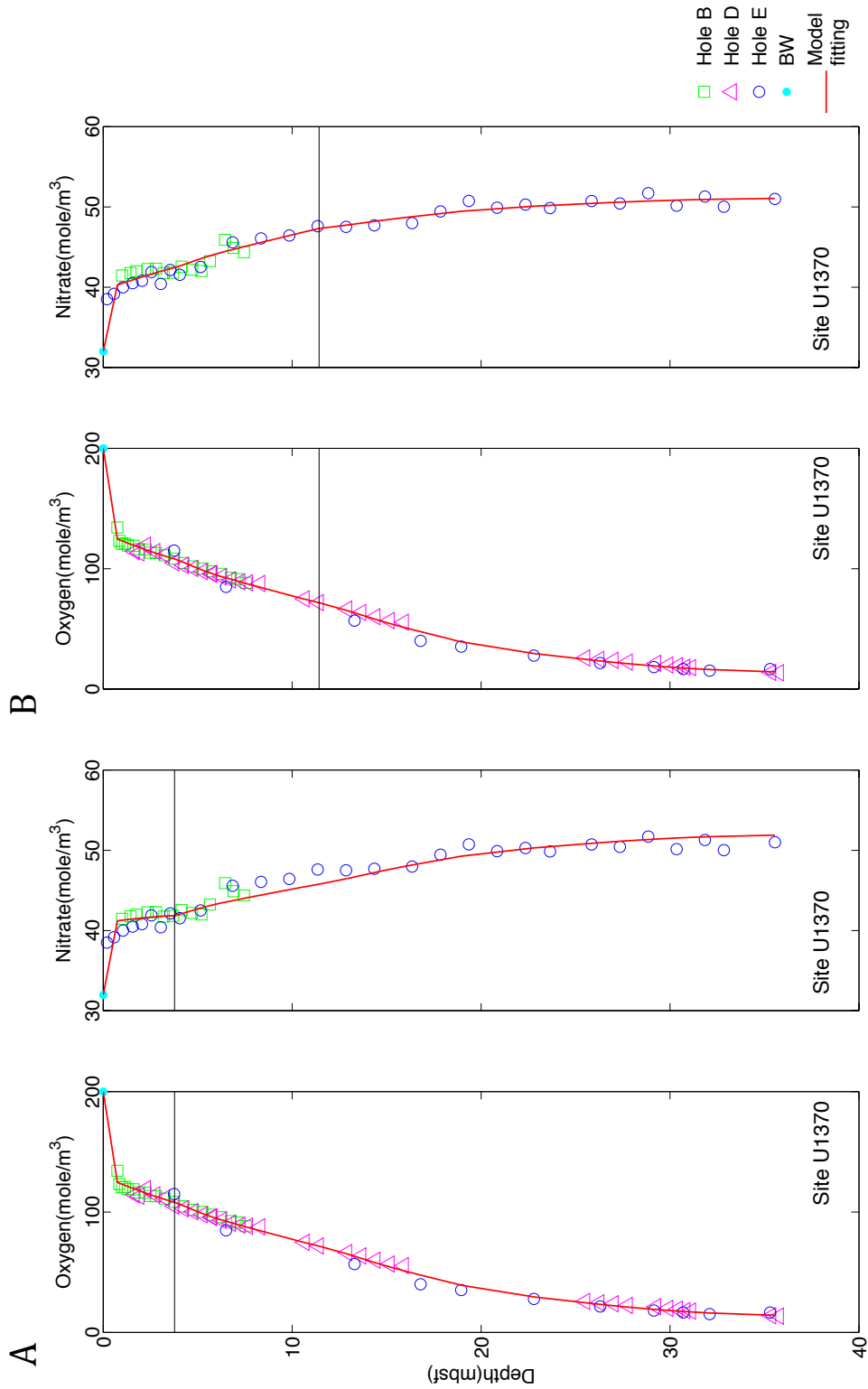


Figure 10.3 The best-fit oxygen and nitrate curves from the two-zone model at Site U1370. Measured depth of Hole E is used. The solid horizontal lines indicate the depth where the sediment column is separated. Flux BC is used for the deeper zone.

TABLES

Table 1 The location and water depth of the sediment sample sites.

	Latitude	Longitude	Water depth (mbsf)
Site 10	20°41.0' N	143°21.4' W	5410
Site 11	30°21.3' N	157°52.2' W	5819
Site U 1370	41°51.1' S	153°06.4' W	5074

Table 2 The best-fit NO_3^-/O_2 respiration ratio and the referred C/N ratio from the one-zone model at each site, using both Conc. BC and Flux BC. The uncertainty of NO_3^-/O_2 respiration ratio is of 95% confidence level. The referred C/N is calculated based on the NO_3^-/O_2 respiration ratio and the average carbon oxidation state of 0 (R.K.R, 1963), shown in italics, and -0.7 (Hedges *et al.*, 2002), shown in parenthesis. The C/N/ O_2 ratios from pervious studies are also listed for comparison.

	NO_3^-/O_2	Referred C/N
	Conc. BC	
Site 10	0.089 ± 0.004	<i>9.2</i> (7.9)
Site 11	0.100 ± 0.003	<i>8.0</i> (6.8)
Site U1370	0.098 ± 0.004	<i>8.2</i> (7.0)
Mean	0.096 ± 0.003	<i>8.5</i> (7.2)
	Flux BC	
Site 10	0.094 ± 0.002	<i>8.7</i> (7.4)
Site 11	0.092 ± 0.001	<i>8.9</i> (7.6)
Site U1370	0.090 ± 0.002	<i>9.1</i> (7.8)
Mean	0.092 ± 0.002	<i>8.9</i> (7.6)
Grundmanis & Murray (1982)	0.099 ± 0.015	8.1 ± 2.2
Takahashi <i>et al.</i> (1985)	0.093	6.6 - 8.8
Anderson & Sarmiento (1994)	0.094	7.3

Table 3 The best-fit NO_3^-/O_2 respiration ratios from the two-zone model at each site.

The boundary of two zones is placed at the depth where the change of oxygen concentration is calculated including the bottom water value (r^*) or excluding the bottom water value (r^{**}). Only Conc. BC is used for the upper zone and Conc. BC (A) and Flux BC (B) are considered for the deeper zone.

A			
	Conc. BC		
	One zone	Two zones	
	r	r^*	r^{**}
Site 10	0.089	0.085 0.117	0.086 0.121
Site 11	0.100	0.151 0.075	0.145 0.076
Site U1370	0.098	0.104 0.136	0.089 0.076

B			
	Flux BC		
	One zone	Two zones	
	r	r^*	r^{**}
Site 10	0.094	0.085 0.107	0.086 0.114
Site 11	0.092	0.151 0.067	0.145 0.066
Site U1370	0.090	0.104 0.089	0.089 0.055

APPENDIX

Tables of data

Tables of measured data for Site 10 and Site 11 (data were measured by shipboard scientists of Voyage Knorr 195(III)). Data for IODP Site U1370 are available on IODP Expedition 329 website.

Table 1. The dissolved oxygen concentrations measured at Site 10. Different colors indicate concentrations measured on different cores (Orange: gravity core G1; purple: gravity core G2; green: long piston core L1; blue: long piston core L2; red: multicore MC).

Depth (m)	O ₂ (μM)	Depth (m)	O ₂ (μM)	Depth (m)	O ₂ (μM)
1.1	108.1376391	0.95	112.3299652	11.2	27.17839958
0.6	120.777585	1.25	102.8884999	10.75	28.65548573
0.9	113.623377	1.1	109.8871954	13.71	21.97371968
1.48	96.9466498	0.8	121.499139	23.45	14.52747
0.8	116.8290948	2.48	86.85852061	0.045	145.8093292
0.45	123.9236329	2.03	92.12986132	0.06	143.7187611
0.3	123.9333892	1.73	95.97505421	0.075	142.7395739
0.05	137.0436017	1.43	98.98041169	0.09	141.4420358
0.4	124.7514792	8.44	36.42100017	0.105	139.7492454
0.525	122.9671812	9.75	30.8954543	0.12	138.213195
0.25	123.9867323	1.88	92.43325585	0.135	137.435918
0.7	119.114548	2.18	89.73279124	0.185	132.528924
1	111.6600073	2.33	87.9175482	0.235	128.9245288
1.2	105.8832622	2.63	84.57726105	0.285	127.612825
1.32	102.2466758	2.78	82.88627848	0.26	128.3231327
1.55	95.59470236	11.45	26.47495	0.1	140.856911
1.725	89.88365502	12.75	23.45363075	0.13	134.1211765
1.925	86.1983322	4.25	69.18864634	0.16	131.4258899
2.125	86.63507042	15.75	19.11468686	0.19	129.4818095
2.675	75.60713257	14.45	20.76003388	0.23	127.1048488
2.875	79.13067693	3.85	72.15283182	0.28	125.6961493
3.075	76.83904272	17.45	17.07700657	0.33	123.3433898
3.54	70.26780081	18.425	15.61188514	0.39	122.0538748
1.55	94.71446507	3.28	77.8060593	0.46	119.1232648
2.675	82.24873571	18.94	15.73336437	0.54	118.4618386
2.125	85.5216613	7.275	47.25166662	0.63	115.7506673
3.54	70.26118457	20.25	14.69254696	0.73	113.6413793

Table1. Continued.					
1.725	90.05481049	7.85	42.78529358	0.84	111.1988387
2.875	79.90183294	7.55	44.77420115	0.96	107.7665331
3.075	75.81530446	25.95	13.18444028	1.09	106.9939238
1.925	87.20550221	26.3	12.20711387	1.23	103.595167
0.15	130.3141255	21.42	14.63271819	1.38	100.0003625
1.17	104.3695328	21.42	11.53389514	1.58	95.30233684
1.92	82.08927794	22	11.65101804	1.71	89.62807112
3.69	75.03135136	20.83	12.47807288	1.89	87.1163951
2.93	82.97285049	5.8	55.4865053	2.08	85.41321224
4.23	65.27777286	5.4	58.44546996	0.84	112.6982444
4.98	58.6377545	5.1	61.15981282	2.28	83.28737602
5.76	57.86835063	4.75	64.06020993	2.48	79.65999069
6.51	49.89653601	4.45	66.52829941	2.68	77.15352313
7.29	45.15003197	6.09	49.35659288	2.88	74.6227709
8.29	39.13575692	6.35	51.48954499	3.08	73.45757963
9.32	35.91408901	6.83	48.0859257	3.28	69.85523769
11.88	29.50450407	7.05	46.2875678	3.48	67.1735884
10.35	31.39336649	8.25	39.2798589	3.68	65.54531483
13.91	25.38416711	8.55	37.49707447	3.78	63.99753284
15.94	24.74674314	8.83	36.14530423	1.645	91.93923595
18	18.47321142	9.86	31.3697692	1.8	88.88806888
20.03	16.41728287	9.37	33.4217851	0.84	112.420659
		11.55	26.0514613	1.98	86.75366378

Table 2. The dissolved nitrate concentrations measured at Site 10. Different colors indicate concentrations measured on different cores (Orange: gravity core G1; purple: gravity core G2; green: long piston core L1).

Depth (m)	NO ₃ ⁻ (μM)	Depth (m)	NO ₃ ⁻ (μM)	Depth (m)	NO ₃ ⁻ (μM)
0.075	39.07087892	0.175	39.06956217	9.655	50.65332381
0.275	39.39549536	0.225	40.22792179	10.405	51.82613757
0.475	39.56834644	0.275	39.73611158	11.115	50.8892197
0.675	39.98022924	0.325	40.08868464	11.865	51.55126047
1.025	40.93873553	0.375	40.47781866	14.165	52.12664515
1.225	41.95899789	0.425	40.48580591	14.915	52.50066298
1.375	42.49670408	0.425	38.91193041	15.725	52.72352435
1.625	42.92639405	1.175	41.6379818	16.475	52.71729961
1.825	43.5100615	1.875	43.404207	17.255	52.67330904
2.025	43.86574868	3.435	45.52785069	18.005	52.99550611
2.225	43.85916895	4.185	45.97178131	18.795	53.22739105
2.575	44.1240786	4.985	48.12203298	21.095	52.8330316
2.775	44.41992301	5.735	47.47965815	21.875	53.9556804
2.975	44.69255224	6.545	48.80845529	23.405	53.6584533
3.175	45.00680198	7.295	49.14747499	24.155	53.13392516
0.025	37.92509251	8.095	50.95906007	24.935	52.76743695
0.075	38.49949138	8.845	51.41413257	26.215	53.12041957
0.125	39.38273134	9.655	50.65332381	26.565	52.68194734

Table 3. The dissolved oxygen concentrations measured at Site 11. Different colors indicate concentrations measured on different cores (Orange: gravity core G1; purple: gravity core G2; green: long piston core L1; red: multicore MC).

Depth (m)	O ₂ (μM)	Depth (m)	O ₂ (μM)	Depth (m)	O ₂ (μM)
0.2	111.0867206	5.55	54.38710925	0.1	125.5518778
0.375	105.8311517	5.8	53.73815008	0.125	122.6491453
0.575	101.0613003	6.05	54.13186561	0.15	120.914713
1.1	90.10886482	6.3	52.5137527	0.175	119.4776119
1.185	87.5877602	6.56	51.2878784	0.2	118.5039587
1.475	82.13511188	6.81	51.03350843	0.225	117.5889657
1.35	84.97267511	7.06	50.31790668	0.25	116.4761364
1.575	80.8211581	7.31	49.76977568	0.275	115.2633289
2.135	72.36461559	7.55	49.61864491	0.3	114.5722425
2.3	70.52163262	7.82	48.83273481	0.33	113.5132294
2.4	69.75508401	8.07	48.48999939	0.42	111.2469063
2.925	65.64876841	8.57	47.42339981	0.37	112.3197802
3.05	64.82249938	8.87	47.06791609	0.47	109.7971162
3.185	63.80038172	9.23	46.84886089	0.52	108.7063814
3.35	62.44390855	9.58	45.5983629	0.57	107.3652894
3.475	61.81803375	9.98	45.46746499	0.62	106.722848
3.89	58.08987772	10.38	44.61094694	0.68	105.3065541
3.96	57.37034992	10.78	44.61207867	0.75	103.6777109
4.125	56.6028536	11.18	44.12989813	0.83	102.5881507
4.29	55.70509537	11.63	43.86991883	0.92	100.6292067
0.78	116.7103707	12.13	43.26722246	1.02	99.01535478
1.18	103.6445419	12.64	41.18037971	1.12	98.12288995
1.28	85.54071728	13.14	42.4111622	1.22	95.61363452
1.64	78.68572662	13.64	39.80644438	1.32	94.97923703
1.74	76.91717185	14.2	41.49050085	1.42	94.7492245
1.84	75.372752	14.75	40.83371231	1.6	92.41523998
1.94	74.44032613	15.25	40.2338324	1.7	91.13217283
2.04	73.35423391	15.85	39.84502751	1.8	89.67934109
2.29	87.24009095	16.5	39.07347277	1.9	88.35539128
2.39	72.02966208	17.15	38.94902651	2	87.07002522
2.49	70.04628967	17.85	39.01425661	2.2	84.75515605
2.61	68.97068884	18.63	38.40432393	2.3	83.67962974
2.76	68.17813401	19.38	38.13460875	2.4	83.05524289
2.94	66.99704464	20.16	37.88701104	2.5	81.95782493
3.14	64.66227639	20.91	37.67927246	2.6	81.35456234
3.34	64.36073032	21.69	37.42732062	2.7	79.29766953
3.54	64.36073032	22.44	37.22016307	2.8	78.57419862
3.72	61.23627295	23.22	37.00487626	0.03	138.3117944
3.52	67.92380976	24.02	36.82465126	0.07	133.7650584

Table 3. Continued.

3.92	60.69316051	24.77	36.28120713	0.09	129.344811
4.12	59.8944672	25.52	35.73331266	0.11	128.3128669
4.32	58.89646097	26.27	36.45472729	0.13	126.4621555
4.52	58.40258389	27.02	36.57457025	0.15	125.3902541
4.72	57.23833385	27.83	36.24971424	0.175	124.2989769
4.92	56.06160944	28.58	36.32221367	0.2	122.2065768
5.07	55.57402617	0.05	134.8666887	0.225	121.1269333
5.12	55.89784884	0.075	130.8555284	0.25	120.6663746

Table 4. The dissolved nitrate concentrations measured at Site 11. Different colors indicate concentrations measured on different cores (Orange: gravity core G1; green: long piston core L1; red: multicore MC).

Depth (m)	NO ₃ ⁻ (μM)	Depth (m)	NO ₃ ⁻ (μM)	Depth (m)	NO ₃ ⁻ (μM)
0.125	40.47711946	3.715	46.10758967	18.995	47.28876079
0.475	41.04834829	4.495	46.53803325	19.775	47.35361386
0.675	41.67865929	5.245	45.84360571	20.525	47.35163349
1.025	43.0428976	6.025	46.7655801	21.305	47.45107059
1.275	42.94286213	6.775	47.19314916	22.055	47.25525989
1.425	44.16083385	7.515	47.30043813	22.835	47.04056543
1.675	43.8067209	8.265	46.26759505	23.185	47.29418849
2.225	44.80661281	9.075	46.460973	24.235	46.71289555
2.475	46.23208707	9.825	46.53057279	24.985	47.09998791
2.825	47.34356668	10.575	47.33107226	25.735	47.03391921
3.095	45.08274605	11.325	47.11602129	26.485	47.35418186
3.275	45.15912707	12.135	46.78353115	27.195	46.77738011
3.425	46.04248273	12.885	46.74475443	27.645	46.61693338
3.825	45.63299225	13.635	46.88381624	0.025	39.94460638
4.025	46.03287363	14.385	47.17483877	0.125	40.62591593
4.225	46.61404442	15.185	47.75716324	0.175	40.97616424
0.675	41.0074996	15.935	47.36204746	0.275	40.9997366
1.435	44.6021767	16.715	47.11771236	0.325	42.395327
2.185	44.46017131	17.465	47.38080883	0.375	40.34864028
2.965	45.79168795	18.245	46.83589745	0.415	42.27435827

MATLAB code

A. MATLAB code for calculating the best-fit $\text{NO}_3^-/\text{-O}_2$ respiration ratio in one-zone case, with a constant ratio in the entire depth interval analyzed (Example of Site 10).

More information will be available via contacting the author.

A.1 Conc. BC:

```
%% MATLAB code for the calculation of the best-fit NO3-/-O2
% respiration ratio
% One-zone case:
% With a constant ratio throughout the depth interval analyzed
% Example of Site 10
% by Yiya Huang (2013)

% clear the work space
clear all;
close all;

% load data from all sediment cores
data = load('O2_10cutbw.txt');
depth_O2 = data(:,1);
O2_raw = data(:,2);
data = load('NO3_10cutbw.txt');
depth_NO3 = data(:,1);
NO3_raw = data(:,2);

% load data from each sediment core
GC = load('O2_10GC.txt');
GC_OD = GC(:,1);
GC_O = GC(:,2);
LC = load('O2_10LC.txt');
LC_OD = LC(:,1);
LC_O = LC(:,2);
MC = load('O2_10MC.txt');
MC_OD = MC(:,1);
MC_O = MC(:,2);

GC = load('NO3_10GC.txt');
GC_ND = GC(:,1);
GC_N = GC(:,2);
LC = load('NO3_10LC.txt');
LC_ND = LC(:,1);
LC_N = LC(:,2);

% create a depth from zero to 14.15 mbsf, with an even depth interval
of
% 0.025 m
Depth_ini = 0;
Depth_end = 14.15;
Depth_delta = 0.025;
```

```

even_depth = (Depth_ini:Depth_delta:Depth_end)';
num_even = length(even_depth);

% calculate non-dimension depth by dividing each depth by max-depth
NDdepth = even_depth./Depth_end;
delta_nddepth = NDdepth(2)-NDdepth(1);

% smooth oxygen measured data and save in the variable O2
% using LOESS smoothing method
% the bottom water value is not included in smoothing

O2 = zeros(length(depth_O2),1);
O2(1) = O2_raw(1);
O2(2:end) = smooth(depth_O2(2:end),O2_raw(2:end),0.5,'loess');

% smooth nitrate measured data and save in the variable NO3s
% using LOESS smoothing method
% the bottom water value is not included in smoothing

NO3s = zeros(length(depth_NO3),1);
NO3s(1) = NO3_raw(1);
NO3s(2:end) = smooth(depth_NO3(2:end),NO3_raw(2:end),0.5,'loess');

% calculate O2 at even_depth using linear intropolation

% first, pre-allocate a variable for O2_even to store the
interpolating
% oxygen data at even depth
O2_even = zeros(num_even,1);

% same concentration at depth zero (bottom water value)
O2_even(1) = O2(1);

% create a loop to interpolate oxygen concentration into even depth
    k=2;
    for i = 2:num_even
        k = k-1;
        while even_depth(i) > depth_O2(k)
            k = k+1;
        end
        O2_even(i) = O2(k-1) + (O2(k) - O2(k-1)) * (even_depth(i) -
depth_O2(k-1))/(depth_O2(k) - depth_O2(k-1));
    end

% calculate NO3 at even_depth using linear intropolation
NO3_even = zeros(num_even,1);

% same concentration at depth zero
NO3_even(1) = NO3_raw(1);

% create a loop to interpolate nitrate concentration into even depth
    l=2;
    for j = 2:num_even
        l = l-1;
        while even_depth(j) > depth_NO3(l)
            l = l+1;

```

```

        end
        NO3_even(j) = NO3_raw(l-1) + (NO3_raw(l) - NO3_raw(l-1)) *
(even_depth(j) - depth_NO3(l-1))/(depth_NO3(l) - depth_NO3(l-1));
    end

% calculate O2 consumption rate at even_depth
R_O2_raw = zeros(num_even-2,1);

for m = 1:num_even-2
    R_O2_raw(m) = (O2_even(m+2) - 2*O2_even(m+1) +
O2_even(m))/(delta_nddepth.^2);
end

% assign the ratio of DO2/DNO3 (reference: Grundmanis & Murray, 1982)
Dratio = 1.22;

% create concentration column for boundary condition
C_O2 = zeros(num_even-2,1);
C_O2(1) = O2_even(1);
C_O2(num_even-2) = O2_even(num_even);

% calculate O2 * ND_depth^2 - C
DO2 = R_O2_raw .* delta_nddepth^2 - C_O2;

% create matrix A for the calculation in finite difference
A = zeros(num_even-2);
A(logical(eye(size(A))))=-2;
A(1,2) = 1;
A(num_even-2,num_even-3) = 1;

for i=2:num_even-3
    A(i,i-1) = 1;
    A(i,i+1) = 1;
end

% calculated predicted O2 concentration
O2_cal = zeros(num_even,1);
O2_cal(1) = O2_even(1);
O2_cal(end) = O2_even(end);
O2_cal(2:num_even-1) = inv(A) * DO2;

% plot predicted O2 profile vs. measured O2 profile
figure(1);
subplot(1,2,1);
plot(O2_cal.*1000, even_depth, 'r-', 'LineWidth', 1.4);
hold on;
plot(GC_O,GC_OD, 'gs', 'MarkerSize', 10);
hold on;
plot(LC_O,LC_OD, 'bo', 'MarkerSize', 8);
hold on;
plot(MC_O,MC_OD, 'm^', 'MarkerSize', 10);
hold on;
plot(160,0, 'c.', 'MarkerSize', 18);
set(gca, 'YDir', 'reverse');
set(gca, 'XAxisLocation', 'top');
set(gca, 'Ytick', 0:10:40);

```

```

xlabel('Oxygen(\muM)', 'FontSize', 14);
ylabel('Depth(mbsf)', 'FontSize', 14);
text(140, 14.5, 'Site 10', 'Color', 'k', 'FontSize', 15);
set(gcf, 'Position', [300 300 300 600]);

% create an adjustable parameter r, which represents the NO3-/-O2
% respiration ratio

% define C_No3
C_NO3 = zeros(num_even-2, 1);
C_NO3(1) = NO3_even(1);
C_NO3(end) = NO3s(end);

Flag = true;
r0 = -0.09;
r = zeros(1, 6);
count1 = 0;
count2 = 0;

while Flag == true

    r(1) = r0;
    r(2) = 1.01*r0;
    r(3) = 1.02*r0;
    r(4) = 1.03*r0;
    r(5) = 1.04*r0;
    r(6) = 1.05*r0;

    % calculate R(NO3)
    R0_NO3 = R_O2_raw .* Dratio * r(1);
    R1_NO3 = R_O2_raw .* Dratio * r(2);
    R2_NO3 = R_O2_raw .* Dratio * r(3);
    R3_NO3 = R_O2_raw .* Dratio * r(4);
    R4_NO3 = R_O2_raw .* Dratio * r(5);
    R5_NO3 = R_O2_raw .* Dratio * r(6);

    % calculate R_NO3* delta_depth^2 - C
    DR0_NO3 = R0_NO3.* delta_nddepth.^2 - C_NO3;
    DR1_NO3 = R1_NO3.* delta_nddepth.^2 - C_NO3;
    DR2_NO3 = R2_NO3.* delta_nddepth.^2 - C_NO3;
    DR3_NO3 = R3_NO3.* delta_nddepth.^2 - C_NO3;
    DR4_NO3 = R4_NO3.* delta_nddepth.^2 - C_NO3;
    DR5_NO3 = R5_NO3.* delta_nddepth.^2 - C_NO3;

    % calculate calculated NO3 concentration
    NO3_cal = zeros(num_even-2, 6);
    NO3_cal(:, 1) = inv(A) * DR0_NO3;
    NO3_cal(:, 2) = inv(A) * DR1_NO3;
    NO3_cal(:, 3) = inv(A) * DR2_NO3;
    NO3_cal(:, 4) = inv(A) * DR3_NO3;
    NO3_cal(:, 5) = inv(A) * DR4_NO3;
    NO3_cal(:, 6) = inv(A) * DR5_NO3;

    % combine two boundary point into calculated NO3 data
    NO3_p = zeros(num_even, 6);

```

```

NO3_p(1,:) = NO3_raw(1);
NO3_p(num_even,:) = NO3s(end);
NO3_p(2:num_even-1,:) = NO3_cal;

% calculate SSE
NO3_r = zeros(length(depth_NO3)-1,6);
NO3_r(1,:) = NO3_raw(1);

for j = 1:6
    l=2;
    for i = 2:(length(depth_NO3)-1)
        l = l-1;
        while depth_NO3(i) > even_depth(l)
            l = l+1;
        end
        NO3_r(i,j) = NO3_p(l-1,j) + (NO3_p(l,j) -
NO3_p(l-1,j)) * (depth_NO3(i) - even_depth(l-1))/(even_depth(l) -
even_depth(l-1));
    end
end

SSE(1) = sum((NO3_raw(1:end-1) - NO3_r(:,1)).^2);
SSE(2) = sum((NO3_raw(1:end-1) - NO3_r(:,2)).^2);
SSE(3) = sum((NO3_raw(1:end-1) - NO3_r(:,3)).^2);
SSE(4) = sum((NO3_raw(1:end-1) - NO3_r(:,4)).^2);
SSE(5) = sum((NO3_raw(1:end-1) - NO3_r(:,5)).^2);
SSE(6) = sum((NO3_raw(1:end-1) - NO3_r(:,6)).^2);

min_SSE = min(SSE);

if min_SSE == SSE(1)
    r0 = r0/1.05;
    disp(1);
    Flag = true;
    count1 = count1+1;
elseif min_SSE == SSE(6)
    count2 = count2+1;
    if count1 >2 && count2 >2
        Flag = false;
        best = 6;
    else r0 = r(6);
        disp(2);
        Flag = true;
    end
elseif min_SSE == SSE(2)
    best = 2;
    Flag = false;
elseif min_SSE == SSE(3)
    best = 3;
    Flag = false;
elseif min_SSE == SSE(4)
    best = 4;
    Flag = false;
elseif min_SSE == SSE(5)
    best = 5;
    Flag = false;
end
end

```

```

end

% display the best-fit NO3-/-O2 respiration ratio
rbest = r(best);
disp(rbest);
fprintf('data points: %d\n',length(depth_NO3));
disp('SSE = ');
disp(SSE(best));
% plot the predicted nitrate profile (based on the best-fit NO3-/-O2
% respiration ratio)versus the measured nitrate profile

figure(1);
subplot(1,2,2);
plot(NO3_p(:,best).*1000, even_depth,'r','LineWidth',1.1);
hold on;
plot(GC_N,GC_ND,'gs','MarkerSize',10);
hold on;
plot(LC_N,LC_ND,'bo','MarkerSize',8);
hold on;
plot(36,0,'c.','MarkerSize',18);
set(gca,'YDir','reverse');
set(gca,'XAxisLocation','top');
xlim([30 60]);
set(gca,'Ytick',0:10:40);
set(gca,'YTickLabelMode','manual','YTickLabel',[]);
xlabel('Nitrate(\muM)','FontSize',14);
text(32, 14.5, 'Site 10', 'Color','k','FontSize',15);
set(gcf,'Position',[300 300 600 700]);
set(gcf,'color','w');

```

A.2 Flux BC:

```
%% MATLAB code for the calculation of the best-fit NO3-/-O2
respiration ratio
% One-zone case:
% with a constant ratio throughout the depth interval analyzed
% Example of Site 10
% by Yiya Huang (2013)

% clear the work space
clear all;
close all;

% load data from all sediment cores
data = load('O2_10cutbw.txt');
depth_O2 = data(:,1);
O2_raw = data(:,2);
data = load('NO3_10cutbw.txt');
depth_NO3 = data(:,1);
NO3_raw = data(:,2);

% load data from each sediment core
GC = load('O2_10GC.txt');
GC_OD = GC(:,1);
GC_O = GC(:,2);
LC = load('O2_10LC.txt');
LC_OD = LC(:,1);
LC_O = LC(:,2);
MC = load('O2_10MC.txt');
MC_OD = MC(:,1);
MC_O = MC(:,2);

GC = load('NO3_10GC.txt');
GC_ND = GC(:,1);
GC_N = GC(:,2);
LC = load('NO3_10LC.txt');
LC_ND = LC(:,1);
LC_N = LC(:,2);

% create a depth from zero to 14.15 mbsf, with an even depth interval
of
% 0.025 m

Depth_ini = 0;
Depth_end = 14.15;
Depth_delta = 0.025;

even_depth = (Depth_ini:Depth_delta:Depth_end)';
num_even = length(even_depth);

% calculate non-dimension depth by dividing each depth by max-depth
NDdepth = even_depth./Depth_end;
delta_nddepth = NDdepth(2)-NDdepth(1);
```

```

% smooth oxygen measured data and save in the variable O2
% using LOESS smoothing method
% the bottom water value is not included in smoothing

O2 = zeros(length(depth_O2),1);
O2(1) = O2_raw(1);
O2(2:end) = smooth(depth_O2(2:end),O2_raw(2:end),0.5,'loess');

% smooth nitrate measured data and save in the variable NO3s
% using LOESS smoothing method
% the bottom water value is not included in smoothing

NO3s = zeros(length(depth_NO3),1);
NO3s(1) = NO3_raw(1);
NO3s(2:end) = smooth(depth_NO3(2:end),NO3_raw(2:end),0.5,'loess');

% calculate O2 at even_depth using linear intropolation

% first, pre-allocate a variable for O2_even to store the
interpolating
% oxygen data at even depth
O2_even = zeros(num_even,1);

% same concentration at depth zero (bottom water value)
O2_even(1) = O2(1);

% create a loop to interpolate oxygen concentration into even depth
    k=2;
    for i = 2:num_even
        k = k-1;
        while even_depth(i) > depth_O2(k)
            k = k+1;
        end
        O2_even(i) = O2(k-1) + (O2(k) - O2(k-1)) * (even_depth(i) -
depth_O2(k-1))/(depth_O2(k) - depth_O2(k-1));
    end

% calculate NO3 at even_depth using linear intropolation
NO3_even = zeros(num_even,1);

% same concentration at depth zero
NO3_even(1) = NO3_raw(1);

% create a loop to interpolate nitrate concentration into even depth
    l=2;
    for j = 2:num_even
        l = l-1;
        while even_depth(j) > depth_NO3(l)
            l = l+1;
        end
        NO3_even(j) = NO3_raw(l-1) + (NO3_raw(l) - NO3_raw(l-1)) *
(even_depth(j) - depth_NO3(l-1))/(depth_NO3(l) - depth_NO3(l-1));
    end

```

```

% calculate O2 consumption rate at even_depth
R_O2_raw = zeros(num_even-2,1);

for m = 1:num_even-2
    R_O2_raw(m) = (O2_even(m+2) - 2*O2_even(m+1) +
O2_even(m))/(delta_nddepth.^2);
end

% assign the ratio of DO2/DNO3 (reference: Grundmanis & Murray, 1982)
Dratio = 1.22;

% create concentration column for boundary condition
C_O2 = zeros(num_even-2,1);
C_O2(1) = O2_even(1);

% calculate O2 * ND_depth^2 - C
DO2 = zeros(num_even-1,1);
DO2(1:end-1) = R_O2_raw .* delta_nddepth^2 - C_O2;
DO2(end) = O2_even(end-1)-O2_even(end);

% create matrix A for the calculation of finite difference
A = zeros(num_even-1);
A(logical(eye(size(A))))=-2;
A(1,2) = 1;

for i=2:num_even-2
    A(i,i-1) = 1;
    A(i,i+1) = 1;
end
A(num_even-1,num_even-2) = 1;
A(num_even-1,num_even-1) = -1;

% calculate the predicted O2 concentration
O2_cal = zeros(num_even,1);
O2_cal(1) = O2_even(1);
O2_cal(2:num_even) = inv(A) * DO2;

% plot predicted oxygen profile vs. measured oxygen profile
O2_cal = O2_cal.*1000;
O2_raw = O2_raw.*1000;
figure(1);
subplot(1,2,1);
plot(O2_cal, even_depth, 'r-', 'LineWidth',1.1);
hold on;
plot(GC_O,GC_OD, 'gs', 'MarkerSize',10);
hold on;
plot(LC_O,LC_OD, 'bo', 'MarkerSize',8);
hold on;
plot(MC_O,MC_OD, 'm^', 'MarkerSize',10);
hold on;
plot(160,0, 'c.', 'MarkerSize',18);
set(gca, 'YDir', 'reverse');
set(gca, 'XAxisLocation', 'top');
xlabel('Oxygen(\muM)', 'FontSize',14);

```

```

ylabel('Depth(mbsf)', 'FontSize', 14);
text(140, 14.5, 'Site 10', 'Color', 'k', 'FontSize', 15);

% create an adjustable parameter r, which represents the N/-O2
% respiration ratio

% define C_NO3
C_NO3 = zeros(num_even-2,1);
C_NO3(1) = NO3_even(1);

Flag = true;
r0 = -0.09;
r = zeros(1,6);
count1 = 0;
count2 = 0;

while Flag == true

    r(1) = r0;
    r(2) = 1.01*r0;
    r(3) = 1.02*r0;
    r(4) = 1.03*r0;
    r(5) = 1.04*r0;
    r(6) = 1.05*r0;

    % calculate R(NO3)
    R0_NO3 = R_O2_raw .* Dratio * r(1);
    R1_NO3 = R_O2_raw .* Dratio * r(2);
    R2_NO3 = R_O2_raw .* Dratio * r(3);
    R3_NO3 = R_O2_raw .* Dratio * r(4);
    R4_NO3 = R_O2_raw .* Dratio * r(5);
    R5_NO3 = R_O2_raw .* Dratio * r(6);

    % calculate R_NO3* delta_depth^2 - C
    DR0_NO3 = zeros(num_even-1,1);
    DR0_NO3(1:end-1) = R0_NO3.* delta_nddepth.^2 - C_NO3;
    DR0_NO3(end) = DO2(end)*r(1);
    DR1_NO3 = zeros(num_even-1,1);
    DR1_NO3(1:end-1) = R1_NO3.* delta_nddepth.^2 - C_NO3;
    DR1_NO3(end) = DO2(end)*r(2);
    DR2_NO3 = zeros(num_even-1,1);
    DR2_NO3(1:end-1) = R2_NO3.* delta_nddepth.^2 - C_NO3;
    DR2_NO3(end) = DO2(end)*r(3);
    DR3_NO3 = zeros(num_even-1,1);
    DR3_NO3(1:end-1) = R3_NO3.* delta_nddepth.^2 - C_NO3;
    DR3_NO3(end) = DO2(end)*r(4);
    DR4_NO3 = zeros(num_even-1,1);
    DR4_NO3(1:end-1) = R4_NO3.* delta_nddepth.^2 - C_NO3;
    DR4_NO3(end) = DO2(end)*r(5);
    DR5_NO3 = zeros(num_even-1,1);
    DR5_NO3(1:end-1) = R5_NO3.* delta_nddepth.^2 - C_NO3;
    DR5_NO3(end) = DO2(end)*r(6);

    % calculate calculated NO3 concentration

```

```

NO3_cal = zeros(num_even-1,6);
NO3_cal(:,1) = inv(A) * DR0_NO3;
NO3_cal(:,2) = inv(A) * DR1_NO3;
NO3_cal(:,3) = inv(A) * DR2_NO3;
NO3_cal(:,4) = inv(A) * DR3_NO3;
NO3_cal(:,5) = inv(A) * DR4_NO3;
NO3_cal(:,6) = inv(A) * DR5_NO3;

% combine two boundary point into calculated NO3 data
NO3_p = zeros(num_even,6);
NO3_p(1,:) = NO3_raw(1);
NO3_p(2:end,:) = NO3_cal;

% calculate SSE
NO3_r = zeros(length(depth_NO3)-1,6);
NO3_r(1,:) = NO3_raw(1);

for j = 1:6
    l=2;
    for i = 2:(length(depth_NO3)-1)
        l = l-1;
        while depth_NO3(i) > even_depth(l)
            l = l+1;
        end
        NO3_r(i,j) = NO3_p(l-1,j) + (NO3_p(l,j) -
NO3_p(l-1,j)) * (depth_NO3(i) - even_depth(l-1))/(even_depth(l) -
even_depth(l-1));
    end
end

SSE(1) = sum((NO3_raw(1:end-1) - NO3_r(:,1)).^2);
SSE(2) = sum((NO3_raw(1:end-1) - NO3_r(:,2)).^2);
SSE(3) = sum((NO3_raw(1:end-1) - NO3_r(:,3)).^2);
SSE(4) = sum((NO3_raw(1:end-1) - NO3_r(:,4)).^2);
SSE(5) = sum((NO3_raw(1:end-1) - NO3_r(:,5)).^2);
SSE(6) = sum((NO3_raw(1:end-1) - NO3_r(:,6)).^2);

min_SSE = min(SSE);

if min_SSE == SSE(1)
    r0 = r0/1.05;
    disp(1);
    Flag = true;
    count1 = count1+1;
elseif min_SSE == SSE(6)
    count2 = count2+1;
    if count1 >2 && count2 >2
        Flag = false;
        best = 6;
    else r0 = r(6);
        disp(2);
        Flag = true;
    end
elseif min_SSE == SSE(2)
    best = 2;
    Flag = false;
elseif min_SSE == SSE(3)

```

```

        best = 3;
        Flag = false;
    elseif min_SSE == SSE(4)
        best = 4;
        Flag = false;
    elseif min_SSE == SSE(5)
        best = 5;
        Flag = false;
    end
end

end

% display the best-fit NO3-/-O2 respiration ratio and the SSE
rbest = r(best);
disp(rbest);
fprintf('data points: %d\n',num_even);
disp('SSE = ');
disp(SSE(best));

NO3_p = NO3_p.*1000;
NO3_raw = NO3_raw .*1000;

% plot predicted nitrate profile, which is based on the best-fit
% NO3-/-O2 respiration ratio versus measured nitrate profile
figure(1);
subplot(1,2,2);
plot(NO3_p(:,best), even_depth,'r-','LineWidth',1.1);
hold on;
plot(GC_N,GC_ND,'gs','MarkerSize',10);
hold on;
plot(LC_N,LC_ND,'bo','MarkerSize',8);
hold on;
plot(36,0,'c.','MarkerSize',18);
set(gca,'YDir','reverse');
set(gca,'XAxisLocation','top');
xlim([30 60]);
set(gca,'YTickLabelMode','manual','YTickLabel',[]);
xlabel('Nitrate(\muM)','FontSize',14);
text(32, 14.5, 'Site 10', 'Color', 'k','FontSize',15);
set(gcf,'Position',[300 300 600 700]);
set(gcf,'color','w');

```

B. MATLAB code for calculating the best-fit NO_3^-/O_2 respiration ratio in two-zone case, with constant ratio in each zone (Example of Site 10):

```
%% MATLAB code for the calculation of the best-fit NO3-/-O2
respiration ratio
% Two-zone case:
% with independent constant ratio at each zone
% Example of Site 10
% by Yiya Huang (2013)

% clear the work space
clear all;
close all;

% load data from all sediment cores
data = load('O2_10cutbw.txt');
depth_O2 = data(:,1);
O2_raw = data(:,2);
data = load('NO3_10cutbw.txt');
depth_NO3 = data(:,1);
NO3_raw = data(:,2);

% load data from each sediment core
GC = load('O2_10GC.txt');
GC_OD = GC(:,1);
GC_O = GC(:,2);
LC = load('O2_10LC.txt');
LC_OD = LC(:,1);
LC_O = LC(:,2);
MC = load('O2_10MC.txt');
MC_OD = MC(:,1);
MC_O = MC(:,2);

GC = load('NO3_10GC.txt');
GC_ND = GC(:,1);
GC_N = GC(:,2);
LC = load('NO3_10LC.txt');
LC_ND = LC(:,1);
LC_N = LC(:,2);

% smooth oxygen measured data and save in the variable O2
% using LOESS smoothing method
% the bottom water value is not included in smoothing

O2 = zeros(length(depth_O2),1);
O2(1) = O2_raw(1);
O2(2:end) = smooth(depth_O2(2:end),O2_raw(2:end),0.5,'loess');

% create a depth from zero to 14.15 mbsf, with an even depth interval
of
% 0.025 m

Depth_ini = 0;
```

```

Depth_end = 14.15;
Depth_delta = 0.025;

even_depth = (Depth_ini:Depth_delta:Depth_end)';
num_even = length(even_depth);

% calculate non-dimension depth by dividing each depth by max-depth
NDdepth = even_depth./Depth_end;
delta_nddepth = NDdepth(2)-NDdepth(1);

% find out the boundary between two zones

% if include the bottom water value when calculating the changes of
oxygen
% concentration, then use the code:
O2_med = O2(1) - 0.5*(O2(1) - O2(end));
[min,index] = min(abs(O2_med - O2_raw));

% if not include the bottom water value when calculating the changes
of
% oxygen concentration, then use the code:
% O2_med = O2(2) - 0.5*(O2(2) - O2(end));
% [min,index] = min(abs(O2_med - O2_raw));

%%% zone 1
% set the boudnary condition using Conc. BC
Depth_ini_1 = Depth_ini;
temp = even_depth(even_depth > depth_O2(index));
Depth_end_1 = temp(1);
count =1;

% Use function bestfitConcBw2 for upper zone with both Conc. BC
and Flux BC
disp('The best-fit respiration ratio for zone 1 is:')
[even_depth,O2_even,O2_cal,NO3_even,NO3_p,ratio] =
bestfitConcBw2(depth_O2,O2,depth_NO3,NO3_raw,Depth_ini_1,Depth_end_1,
Depth_delta,count);
count = count+3;

% store the variables from the function for zone 1
num_1 = length(even_depth);
zone1 = zeros(num_1,5);
zone1(:,1) = even_depth; % depth
zone1(:,2) = O2_even.*1000; % O2 measured smooth
zone1(:,3) = O2_cal.*1000; % O2 predict
zone1(:,4) = NO3_even.*1000; % NO3 measured
zone1(:,5) = NO3_p.*1000; % NO3 predict

%%% zone 2
% set the boudnary condition using Conc. BC
Depth_ini_2 = Depth_end_1;
Depth_end_2 = Depth_end;

% For Conc. BC, use function bestfitConc2 for the deeper zone,
code

```

```

    % like this:
    disp('The best-fit respiration ratio for zone 2 is:')
    [even_depth,O2_even,O2_cal,N03_even,N03_p,ratio] =
bestfitConc2(depth_O2,O2,depth_NO3,N03_raw,Depth_ini_2,Depth_end_2,De
pth_delta,2);
    count = count+3;
    % For Flux BC, use function bestfitFluxBw2 for the deeper zone,
code
    % like this:
    disp('The best-fit respiration ratio for zone 2 is:')
    [even_depth,O2_even,O2_cal,N03_even,N03_p,ratio] =
bestfitFluxBw2(depth_O2,O2,depth_NO3,N03_raw,Depth_ini_2,Depth_end_2,
Depth_delta,2);
    count = count+3;

    % store the variables from the function for zone 2
    num_2 = length(even_depth);
    zone2 = zeros(num_2,5);
    zone2(:,1) = even_depth;      % depth
    zone2(:,2) = O2_even.*1000;   % O2 measured smooth
    zone2(:,3) = O2_cal.*1000;    % O2 predict
    zone2(:,4) = N03_even.*1000;  % N03 measured
    zone2(:,5) = N03_p.*1000;    % N03 predict

%% combine two zones and plot
two_zone = cat(1,zone1,zone2);
O2_raw = O2_raw.*1000;
N03_raw = N03_raw.*1000;

% plot predicted O2 profile vs. measured O2 profile
figure(1);clf;
subplot(1,4,1);
plot(GC_O,GC_OD,'gs','MarkerSize',10);
hold on;
plot(LC_O,LC_OD,'bo','MarkerSize',8);
hold on;
plot(MC_O,MC_OD,'m^','MarkerSize',10);
hold on;
plot(160,0,'c.','MarkerSize',18);
hold on;
plot(two_zone(:,3),two_zone(:,1),'r-','LineWidth',1.1);
set(gca,'YDir','reverse');
set(gca,'XAxisLocation','top');
xlabel('Oxygen(\muM)','FontSize',14);
ylabel('Depth(mbsf)','FontSize',14);
text(140, 14, 'Site 10', 'Color', 'k','FontSize',15);
hold on;
plot([0 200],[Depth_end_1 Depth_end_1],'k-');
set(gcf,'color','w');
set(gcf,'Position',[100 100 1100 600]);
legend('GC','LC','MC','BW','Model fitting');

% plot the predicted nitrate profile (based on the best-fit N03--O2
% respiration ratio for each zone)versus the measured nitrate profile
figure(1);
subplot(1,4,2);
plot(GC_N,GC_ND,'gs','MarkerSize',10);

```

```

hold on;
plot(LC_N,LC_ND,'bo','MarkerSize',8);
hold on;
plot(36,0,'c.','MarkerSize',18);
hold on;
plot(two_zone(:,5),two_zone(:,1),'r-','LineWidth',1.1);
set(gca,'YDir','reverse');
set(gca,'XAxisLocation','top');
xlim([30 60]);
xlabel('Nitrate(\muM)','FontSize',14);
set(gca,'YTickLabelMode','manual','YTickLabel',[]);
text(33,14,'Site 10','Color','k','FontSize',15);
hold on;
plot([30 60],[Depth_end_1 Depth_end_1],'k-');
set(gcf,'color','w');

```

Function bestfitConcBw2:

```

function [even_depth,O2_even,O2_cal,N03_even,N03_p,rbest] =
bestfitConc2(depth_O2,O2,depth_N03,N03_raw,Depth_ini,Depth_end,Depth_
delta,choice)
% input data:
% depth_O2, O2_raw, depth_N03, N03_raw --> original measured data
% Depth_ini,Depth_end,Depth_delta --> create even depth
% count --> index of plots

% create even depth
even_depth = (Depth_ini:Depth_delta:Depth_end)';
num_even = length(even_depth);

% calculate non-dimension depth
NDdepth = even_depth./Depth_end;
delta_nddepth = NDdepth(2)-NDdepth(1);

% calculate O2 at even_depth using linear intropolation
O2_even = zeros(num_even,1);

k=2;
for i = 1:num_even
    k = k-1;
    while even_depth(i) > depth_O2(k)
        k = k+1;
    end
    O2_even(i) = O2(k-1) + (O2(k) - O2(k-1)) * (even_depth(i) -
depth_O2(k-1))/(depth_O2(k) - depth_O2(k-1));
end

% calculate N03 at even_depth using linear intropolation
N03_even = zeros(num_even,1);

N03 = zeros(length(depth_N03),1);
N03(1) = N03_raw(1);
N03(2:end) = smooth(depth_N03(2:end),N03_raw(2:end),0.5,'loess');

```

```

index = find(Depth_ini < depth_NO3);
index = index(1);
NO3_even(1) = NO3(index-1)+((NO3(index)-NO3(index-1))*(Depth_ini
- depth_NO3(index-1))/(depth_NO3(index)-depth_NO3(index-1)));

if Depth_end < depth_NO3(end)
    NO3_end = NO3(end-1)+((NO3(end)-NO3(end-1))*(Depth_end -
depth_NO3(end-1))/(depth_NO3(end)-depth_NO3(end-1)));
end

l=2;
for j = 2:num_even
    l = l-1;
    while even_depth(j) > depth_NO3(l)
        l = l+1;
    end
    NO3_even(j) = NO3_raw(l-1) + (NO3_raw(l) - NO3_raw(l-1)) *
(even_depth(j) - depth_NO3(l-1))/(depth_NO3(l) - depth_NO3(l-1));
end

% calculate O2 consumption rate at even_depth
R_O2_raw = zeros(num_even-2,1);

for m = 1:num_even-2
    R_O2_raw(m) = (O2_even(m+2) - 2*O2_even(m+1) +
O2_even(m))/(delta_nddepth.^2);
end

% ratio of DO2/DNO3
Dratio = 1.22;

% create concentration column for boundary condition
C_O2 = zeros(num_even-2,1);
C_O2(1) = O2_even(1);
C_O2(num_even-2) = O2_even(num_even);

% calculate O2 * ND_depth^2 - C
DO2 = R_O2_raw .* delta_nddepth^2 - C_O2;

% create finite difference matrix A
A = zeros(num_even-2);
A(logical(eye(size(A))))=-2;
A(1,2) = 1;
A(num_even-2,num_even-3) = 1;

for i=2:num_even-3
    A(i,i-1) = 1;
    A(i,i+1) = 1;
end

% calculated O2 concentration
O2_cal = zeros(num_even,1);
O2_cal(1) = O2_even(1);
O2_cal(end) = O2_even(end);
O2_cal(2:num_even-1) = inv(A) * DO2;

```

```

% create an adjustable parameter r, which represents the N/-O2
% respiration ratio

% define C_No3
C_NO3 = zeros(num_even-2,1);
C_NO3(1) = NO3_even(1);
if choice ==1
    C_NO3(end) = NO3(end);
elseif choice ==2
    C_NO3(end) = NO3_end;
end

Flag = true;
r0 = -0.09;
r = zeros(1,6);
count1 = 0;
count2 = 0;

while Flag == true

    r(1) = r0;
    r(2) = 1.01*r0;
    r(3) = 1.02*r0;
    r(4) = 1.03*r0;
    r(5) = 1.04*r0;
    r(6) = 1.05*r0;

    % calculate R(NO3)
    R0_NO3 = R_O2_raw .* Dratio * r(1);
    R1_NO3 = R_O2_raw .* Dratio * r(2);
    R2_NO3 = R_O2_raw .* Dratio * r(3);
    R3_NO3 = R_O2_raw .* Dratio * r(4);
    R4_NO3 = R_O2_raw .* Dratio * r(5);
    R5_NO3 = R_O2_raw .* Dratio * r(6);

    % calculate R_NO3* delta_depth^2 - C
    DR0_NO3 = R0_NO3.* delta_nddepth.^2 - C_NO3;
    DR1_NO3 = R1_NO3.* delta_nddepth.^2 - C_NO3;
    DR2_NO3 = R2_NO3.* delta_nddepth.^2 - C_NO3;
    DR3_NO3 = R3_NO3.* delta_nddepth.^2 - C_NO3;
    DR4_NO3 = R4_NO3.* delta_nddepth.^2 - C_NO3;
    DR5_NO3 = R5_NO3.* delta_nddepth.^2 - C_NO3;

    % calculate calculated NO3 concentration
    NO3_cal = zeros(num_even-2,6);
    NO3_cal(:,1) = inv(A) * DR0_NO3;
    NO3_cal(:,2) = inv(A) * DR1_NO3;
    NO3_cal(:,3) = inv(A) * DR2_NO3;
    NO3_cal(:,4) = inv(A) * DR3_NO3;
    NO3_cal(:,5) = inv(A) * DR4_NO3;
    NO3_cal(:,6) = inv(A) * DR5_NO3;

    % case for the largest depth is equal to the max
even_depth
    if choice ==1

```

```

% combine two boundary point into calculated NO3 data
NO3_p = zeros(num_even,6);
NO3_p(1,:) = NO3_even(1);
NO3_p(num_even,:) = NO3(end);
NO3_p(2:num_even-1,:) = NO3_cal;

% calculate SSE
indexd = find(depth_NO3 > Depth_ini);
startp = indexd(1);
maxd = length(depth_NO3(indexd));

NO3_r = zeros(maxd,6);

for j = 1:6
    l=2;

    for i = 1:maxd
        l = l-1;
        while depth_NO3(startp+i-1) > even_depth(l)
            l = l+1;
        end
        if depth_NO3(startp+i-1) == even_depth(l)
            NO3_r(i,j) = NO3_p(l,j);
        else
            NO3_r(i,j) = NO3_p(l-1,j) + ((NO3_p(l,j) -
NO3_p(l-1,j)) * (depth_NO3(startp+i-1) - even_depth(l-
1)))/(even_depth(l) - even_depth(l-1)));
        end
    end
end

%for site 10 & site 11
SSE(1) = sum((NO3_raw(indexd) - NO3_r(:,1)).^2);
SSE(2) = sum((NO3_raw(indexd) - NO3_r(:,2)).^2);
SSE(3) = sum((NO3_raw(indexd) - NO3_r(:,3)).^2);
SSE(4) = sum((NO3_raw(indexd) - NO3_r(:,4)).^2);
SSE(5) = sum((NO3_raw(indexd) - NO3_r(:,5)).^2);
SSE(6) = sum((NO3_raw(indexd) - NO3_r(:,6)).^2);

min_SSE = min(SSE);

if min_SSE == SSE(1)
    r0 = r0/1.05;
    disp(1);
    Flag = true;
    count1 = count1+1;
elseif min_SSE == SSE(6)
    count2 = count2+1;
    if count1 >2 && count2 >2
        Flag = false;
        best = 6;
    else
        r0 = r(6);
        disp(2);
        Flag = true;
    end
end

```

```

        end
    elseif min_SSE == SSE(2)
        best = 2;
        Flag = false;
    elseif min_SSE == SSE(3)
        best = 3;
        Flag = false;
    elseif min_SSE == SSE(4)
        best = 4;
        Flag = false;
    elseif min_SSE == SSE(5)
        best = 5;
        Flag = false;
    end
end
end

% case for the largest depth is inequal to the max
even_depth
if choice ==2
    % combine two boundary point into calculated NO3 data
    NO3_p = zeros(num_even,6);
    NO3_p(1,:) = NO3_even(1);
    NO3_p(num_even,:) = NO3_end;
    NO3_p(2:num_even-1,:) = NO3_cal;

    % calculate SSE
    indexd = find(depth_NO3 > Depth_ini);
    startp = indexd(1);
    maxd = length(depth_NO3(indexd))-1;

    NO3_r = zeros(maxd,6);

    for j = 1:6
        l=2;

        for i = 1:maxd
            l = l-1;
            while depth_NO3(startp+i-1) > even_depth(l)
                l = l+1;
            end
            if depth_NO3(startp+i-1) == even_depth(l)
                NO3_r(i,j) = NO3_p(l,j);
            else
                NO3_r(i,j) = NO3_p(l-1,j) + ((NO3_p(l,j) -
NO3_p(l-1,j)) * (depth_NO3(startp+i-1) - even_depth(l-
1)) / (even_depth(l) - even_depth(l-1)));
            end
        end
    end

    SSE(1) = sum((NO3_raw(indexd(1:end-1)) -
NO3_r(:,1)).^2);
    SSE(2) = sum((NO3_raw(indexd(1:end-1)) -
NO3_r(:,2)).^2);
    SSE(3) = sum((NO3_raw(indexd(1:end-1)) -
NO3_r(:,3)).^2);

```

```

        SSE(4) = sum((NO3_raw(indexd(1:end-1)) -
NO3_r(:,4)).^2);
        SSE(5) = sum((NO3_raw(indexd(1:end-1)) -
NO3_r(:,5)).^2);
        SSE(6) = sum((NO3_raw(indexd(1:end-1)) -
NO3_r(:,6)).^2);

        min_SSE = min(SSE);

        if min_SSE == SSE(1)
            r0 = r0/1.05;
            disp(1);
            Flag = true;
            count1 = count1+1;
        elseif min_SSE == SSE(6)
            count2 = count2+1;
            if count1 >2 && count2 >2
                Flag = false;
                best = 6;
            else r0 = r(6);
                disp(2);
                Flag = true;
            end
        elseif min_SSE == SSE(2)
            best = 2;
            Flag = false;
        elseif min_SSE == SSE(3)
            best = 3;
            Flag = false;
        elseif min_SSE == SSE(4)
            best = 4;
            Flag = false;
        elseif min_SSE == SSE(5)
            best = 5;
            Flag = false;
        end
    end
end

        rbest = r(best);
        disp(rbest);
        fprintf('data points: %d\n',length(depth_NO3));
        disp('SSE = ');
        disp(SSE(best));

        NO3_p = NO3_p(:,best);

end

```

Function bestfitFluxBw2:

```

function [even_depth,O2_even,O2_cal,NO3_even,NO3_p,rbest] =
bestfitFluxBw2(depth_O2,O2,depth_NO3,NO3_raw,Depth_ini,Depth_end,Depth_
h_delta,choice)
% input data:
% depth_O2, O2_raw, depth_NO3, NO3_raw --> original measured data
% Depth_ini,Depth_end,Depth_delta --> create even depth
% count --> index of plots

```

```

% create even depth
even_depth = (Depth_ini:Depth_delta:Depth_end)';
num_even = length(even_depth);

% calculate non-dimension depth
NDdepth = even_depth./Depth_end;
delta_nddepth = NDdepth(2)-NDdepth(1);

% calculate O2 at even_depth using linear intropolation
O2_even = zeros(num_even,1);

k=2;
for i = 1:num_even
    k = k-1;
    while even_depth(i) > depth_O2(k)
        k = k+1;
    end
    O2_even(i) = O2(k-1) + (O2(k) - O2(k-1)) * (even_depth(i) -
depth_O2(k-1))/(depth_O2(k) - depth_O2(k-1));
end

% calculate NO3 at even_depth using linear intropolation
NO3_even = zeros(num_even,1);
NO3 = zeros(length(depth_NO3),1);
NO3(1) = NO3_raw(1);
NO3(2:end) = smooth(depth_NO3(2:end),NO3_raw(2:end),0.5,'loess');

index = find(Depth_ini < depth_NO3);
index = index(1);
NO3_even(1) = NO3(index-1)+((NO3(index)-NO3(index-1))*(Depth_ini
- depth_NO3(index-1))/(depth_NO3(index)-depth_NO3(index-1)));

l=2;
for j = 2:num_even
    l = l-1;
    while even_depth(j) > depth_NO3(l)
        l = l+1;
    end
    NO3_even(j) = NO3_raw(l-1) + (NO3_raw(l) - NO3_raw(l-1)) *
(even_depth(j) - depth_NO3(l-1))/(depth_NO3(l) - depth_NO3(l-1));
end

% calculate O2 consumption rate at even_depth
R_O2_raw = zeros(num_even-2,1);

for m = 1:num_even-2
    R_O2_raw(m) = (O2_even(m+2) - 2*O2_even(m+1) +
O2_even(m))/(delta_nddepth.^2);
end

% ratio of DO2/DNO3
Dratio = 1.22;

% create concentration column for boundary condition

```

```

C_O2 = zeros(num_even-2,1);
C_O2(1) = O2_even(1);

% calculate O2 * ND_depth^2 - C
DO2 = zeros(num_even-1,1);
DO2(1:end-1) = R_O2_raw .* delta_nddepth^2 - C_O2;
DO2(end) = O2_even(end-1)-O2_even(end);

% create finite difference matrix A
A = zeros(num_even-1);
A(logical(eye(size(A))))=-2;
A(1,2) = 1;

for i=2:num_even-2
    A(i,i-1) = 1;
    A(i,i+1) = 1;
end
A(num_even-1,num_even-2) = 1;
A(num_even-1,num_even-1) = -1;

% calculated O2 concentration
O2_cal = zeros(num_even,1);
O2_cal(1) = O2_even(1);
O2_cal(2:num_even) = inv(A) * DO2;

% create an adjustable parameter r, which represents the N/-O2
% respiration ratio

% define C_No3
C_NO3 = zeros(num_even-2,1);
C_NO3(1) = NO3_even(1);

Flag = true;
r0 = -0.09;
r = zeros(1,6);
count1 = 0;
count2 = 0;

while Flag == true

    r(1) = r0;
    r(2) = 1.01*r0;
    r(3) = 1.02*r0;
    r(4) = 1.03*r0;
    r(5) = 1.04*r0;
    r(6) = 1.05*r0;

    % calculate R(NO3)
    R0_NO3 = R_O2_raw .* Dratio * r(1);
    R1_NO3 = R_O2_raw .* Dratio * r(2);
    R2_NO3 = R_O2_raw .* Dratio * r(3);
    R3_NO3 = R_O2_raw .* Dratio * r(4);
    R4_NO3 = R_O2_raw .* Dratio * r(5);
    R5_NO3 = R_O2_raw .* Dratio * r(6);

```

```

% calcualte R_NO3* delta_depth^2 - C
DR0_NO3 = zeros(num_even-1,1);
DR0_NO3(1:end-1) = R0_NO3.* delta_nddepth.^2 - C_NO3;
DR0_NO3(end) = DO2(end)*r(1);
DR1_NO3 = zeros(num_even-1,1);
DR1_NO3(1:end-1) = R1_NO3.* delta_nddepth.^2 - C_NO3;
DR1_NO3(end) = DO2(end)*r(2);
DR2_NO3 = zeros(num_even-1,1);
DR2_NO3(1:end-1) = R2_NO3.* delta_nddepth.^2 - C_NO3;
DR2_NO3(end) = DO2(end)*r(3);
DR3_NO3 = zeros(num_even-1,1);
DR3_NO3(1:end-1) = R3_NO3.* delta_nddepth.^2 - C_NO3;
DR3_NO3(end) = DO2(end)*r(4);
DR4_NO3 = zeros(num_even-1,1);
DR4_NO3(1:end-1) = R4_NO3.* delta_nddepth.^2 - C_NO3;
DR4_NO3(end) = DO2(end)*r(5);
DR5_NO3 = zeros(num_even-1,1);
DR5_NO3(1:end-1) = R5_NO3.* delta_nddepth.^2 - C_NO3;
DR5_NO3(end) = DO2(end)*r(6);

% calculate calculated NO3 concentration
NO3_cal = zeros(num_even-1,6);
NO3_cal(:,1) = inv(A) * DR0_NO3;
NO3_cal(:,2) = inv(A) * DR1_NO3;
NO3_cal(:,3) = inv(A) * DR2_NO3;
NO3_cal(:,4) = inv(A) * DR3_NO3;
NO3_cal(:,5) = inv(A) * DR4_NO3;
NO3_cal(:,6) = inv(A) * DR5_NO3;

% combine two boundary point into calculated NO3 data

NO3_p = zeros(num_even,6);
NO3_p(1,:) = NO3_even(1);
NO3_p(2:end,:) = NO3_cal;

% case for the largest depth is equal to the max
even_depth
if choice ==1

    indexd = find(depth_NO3 > Depth_ini);
    startp = indexd(1);
    maxd = length(depth_NO3(indexd));
% calculate SSE
NO3_r = zeros(maxd,6);

    for j = 1:6
        l=2;

        for i = 1:maxd
            l = l-1;
            while depth_NO3(startp+i-1) > even_depth(l)
                l = l+1;
            end
            if depth_NO3(startp+i-1) == even_depth(l)
                NO3_r(i,j) = NO3_p(l,j);
            else
                NO3_r(i,j) = NO3_p(l-1,j) + ((NO3_p(l,j) -

```

```

NO3_p(l-1,j)) * (depth_NO3(startp+i-1) - even_depth(l-
1))/(even_depth(l) - even_depth(l-1)));
        end
    end
end

SSE(1) = sum((NO3_raw(indexd) - NO3_r(:,1)).^2);
SSE(2) = sum((NO3_raw(indexd) - NO3_r(:,2)).^2);
SSE(3) = sum((NO3_raw(indexd) - NO3_r(:,3)).^2);
SSE(4) = sum((NO3_raw(indexd) - NO3_r(:,4)).^2);
SSE(5) = sum((NO3_raw(indexd) - NO3_r(:,5)).^2);
SSE(6) = sum((NO3_raw(indexd) - NO3_r(:,6)).^2);

min_SSE = min(SSE);

if min_SSE == SSE(1)
    r0 = r0/1.05;
    disp(1);
    Flag = true;
    count1 = count1+1;
elseif min_SSE == SSE(6)
    count2 = count2+1;
    if count1 >2 && count2 >2
        Flag = false;
        best = 6;
    else r0 = r(6);
        disp(2);
        Flag = true;
    end
elseif min_SSE == SSE(2)
    best = 2;
    Flag = false;
elseif min_SSE == SSE(3)
    best = 3;
    Flag = false;
elseif min_SSE == SSE(4)
    best = 4;
    Flag = false;
elseif min_SSE == SSE(5)
    best = 5;
    Flag = false;
end
end

% case for the largest depth is inequal to the max
even_depth
if choice ==2
    % calculate SSE
    indexd = find(depth_NO3 > Depth_ini);
    startp = indexd(1);
    maxd = length(depth_NO3(indexd))-1;

    NO3_r = zeros(maxd,6);

    for j = 1:6
        l=2;

```

```

        for i = 1:maxd
            l = l-1;
            while depth_NO3(startp+i-1) > even_depth(l)
                l = l+1;
            end
            if depth_NO3(startp+i-1) == even_depth(l)
                NO3_r(i,j) = NO3_p(l,j);
            else
                NO3_r(i,j) = NO3_p(l-1,j) + ((NO3_p(l,j) -
NO3_p(l-1,j)) * (depth_NO3(startp+i-1) - even_depth(l-
1)))/(even_depth(l) - even_depth(l-1)));
            end
        end
    end

    SSE(1) = sum((NO3_raw(indexd(1:end-1)) -
NO3_r(:,1)).^2);
    SSE(2) = sum((NO3_raw(indexd(1:end-1)) -
NO3_r(:,2)).^2);
    SSE(3) = sum((NO3_raw(indexd(1:end-1)) -
NO3_r(:,3)).^2);
    SSE(4) = sum((NO3_raw(indexd(1:end-1)) -
NO3_r(:,4)).^2);
    SSE(5) = sum((NO3_raw(indexd(1:end-1)) -
NO3_r(:,5)).^2);
    SSE(6) = sum((NO3_raw(indexd(1:end-1)) -
NO3_r(:,6)).^2);

    min_SSE = min(SSE);

    if min_SSE == SSE(1)
        r0 = r0/1.05;
        disp(1);
        Flag = true;
        count1 = count1+1;
    elseif min_SSE == SSE(6)
        count2 = count2+1;
        if count1 >2 && count2 >2
            Flag = false;
            best = 6;
        else r0 = r(6);
            disp(2);
            Flag = true;
        end
    elseif min_SSE == SSE(2)
        best = 2;
        Flag = false;
    elseif min_SSE == SSE(3)
        best = 3;
        Flag = false;
    elseif min_SSE == SSE(4)
        best = 4;
        Flag = false;
    elseif min_SSE == SSE(5)
        best = 5;
        Flag = false;
    end
end
end

```

```
end

rbest = r(best);
disp(rbest);
fprintf('data points: %d\n',num_even);
disp('SSE = ');
disp(SSE(best));

NO3_p = NO3_p(:,best);
end
```